

University of Memphis

University of Memphis Digital Commons

Electronic Theses and Dissertations

4-21-2014

Fault Ride-Through Capacity Enhancement of Fixed Speed Wind Generator by A Modified Bridge-type Fault Current Limiter

Gilmanur Rashid

Follow this and additional works at: <https://digitalcommons.memphis.edu/etd>

Recommended Citation

Rashid, Gilmanur, "Fault Ride-Through Capacity Enhancement of Fixed Speed Wind Generator by A Modified Bridge-type Fault Current Limiter" (2014). *Electronic Theses and Dissertations*. 884.
<https://digitalcommons.memphis.edu/etd/884>

This Thesis is brought to you for free and open access by University of Memphis Digital Commons. It has been accepted for inclusion in Electronic Theses and Dissertations by an authorized administrator of University of Memphis Digital Commons. For more information, please contact khhgerty@memphis.edu.

FAULT RIDE-THROUGH CAPACITY ENHANCEMENT OF FIXED SPEED WIND
GENERATOR BY A MODIFIED BRIDGE-TYPE FAULT CURRENT LIMITER

by

Gilmanur Rashid

A Thesis

Submitted in Partial Fulfillment of the

Requirements for the Degree of

Master of Science

Major: Electrical and Computer Engineering

The University of Memphis

May 2014

*This thesis is dedicated to my lovely wife and mother who sacrificed and always
provided inspiration for me*

AKNOWLEDGMENTS

I feel very happy to take the pleasure of expressing my heartiest gratitude to my advisor, thesis committee chairman and Electric Power and Energy Systems (EPES) lab director Dr. Mohd Hasan Ali. This work would not be possible without his prudent supervision, apt guideline and incomparable care. He has always appreciated by ideas and given instruction to nurture them.

I would like to thank Dr. Russell Deaton and Dr. John Hochstein to agree to be in my thesis committee. They also helped me by scrutinizing the thesis and providing valuable advice to enrich my thesis.

I would also like to say thanks to my teachers at the University of Memphis for their help and support to enrich my knowledge and vision. I also want to deliver my appreciation to the present and past members of EPES lab for their informative and technical discussions with me as well as their friendly attitude toward me during my research in the lab. I would like to convey special thanks to Md. Maruf Hossain, Ahmed Eid Abu Hussein, Michael Moore Jr., Sagnika Ghosh, M. A. H. Sadi, Md. Kamal Hossain, Riya Saluja, Yang Zhou and Arnab Banik for their informative comments and suggestions during my work at the EPES lab.

And finally, I would like to thank my mother, wife and rest of the family members for encouraging me throughout my studies to achieve success in my life. I would express my sincere gratitude to them.

ABSTRACT

Rashid, Gilmanur. M.S. The University of Memphis. May 2014. Fault Ride-Through Capacity Enhancement of Fixed Speed Wind Generator by a Modified Bridge-Type Fault Current Limiter. Major Professor: Dr. Mohd. Hasan Ali.

Fault Ride-Through (FRT) is a common requirement to abide by grid code all over the world. In this work, to enhance the fault ride-through capability of a fixed speed wind generator system, a modified configuration of Bridge-Type Fault Current Limiter (BFCL) is proposed. To check the effectiveness of the proposed BFCL, its performance is compared with that of the Series Dynamic Braking Resistor (SDBR). A harmonic performance improvement by the proposed method is also analyzed. Three-line-to-ground (3LG), line-to-line (LL) and single-line-to-ground (1LG) faults were applied to one of the double circuit transmission lines connected to the wind generator system. Simulations were carried out using Matlab/Simulink software. Simulation results show that the proposed BFCL is a very effective device to achieve the FRT and suppress fault current that eliminates the need for circuit breaker replacement. Also, the BFCL improves the harmonic performance and helps follow harmonic grid code. Moreover, it was found that the BFCL works better than the SDBR, and has some distinct advantages over the SDBR.

PREFACE

Two papers, that are outcome of my thesis for master's degree, have been used as the foundation of this work. The results from both the papers have been used collectively in Chapters 3 to 8. I have one accepted journal paper which will be published in the next issue of the IEEE Transactions on Energy Conversion.

Another conference article is currently under preparation and to be submitted at the *North American Power Symposium 2014*.

Following is the list of articles used in this document:

- (1) Rashid, G. and Ali, M.H., "A Modified Bridge-Type Fault Current Limiter for Fault Ride-Through Capacity Enhancement of Fixed Speed Wind Generator". *To be published in the next issue of IEEE Transactions on Energy Conversion*.
- (2) Rashid, G. and Ali, M.H., "Enhancement of Fault Ride-Through Capacity of Fixed Speed Wind Generator Using a Modified Bridge-Type Fault Current Limiter for asymmetrical fault". To be submitted at the "*North American Power Symposium 2014*".

TABLE OF CONTENTS

Chapter	Page
I Introduction	1
A. Global Wind Energy Status	2
B. Wind Energy in Future	2
C. Background and Literature Review	4
D. Motivation	8
E. Novelty	9
F. Thesis Organization	10
II Wind Energy Conversion System (WECS) Overview	11
A. Wind Turbine Components.	12
B. Wind Turbine Types	17
1) Axis of Rotation	18
2) Installation Location	20
3) Output Power Scale	20
4) Rotational Speed	22
5) Axis Orientation and Hub	23
C. Drive Train System	25
1) Six-Mass Drive Train Model	26
2) Three-Mass Drive Train Model	27
3) Two-Mass Shaft Model	27
4) One-Mass or Lumped Model	28
D. Speed and Torque Regulation of Wind Turbines	28
E. Generator Types Used in WECS	30
F. Power Electronics in WECS	33
III Fixed Speed Wind Turbine (FSWT) Modeling	38
A. Wind Turbine Modeling	38
B. Wind Generator Modeling	40
IV Test System Model	43
A. Description of Test System under Analysis	43
V Bridge Type Fault Current Limiter (BFCL)	45
A. BFCL Configuration	45
B. BFCL Operation	46
C. BFCL Design Considerations	48
D. BFCL Control Strategy	49
VI Series Dynamic Braking Resistor (SDBR)	51
A. SDBR Configuration	51
B. SDBR Operation	51

C. SDBR Design Considerations	52
D. SDBR Control Strategy	53
VII Simulation Results and Discussions	54
A. Assumptions and Considerations	54
B. Fault Current Suppression and FRT for 3LG Fault	55
C. Fault Current Suppression and FRT for LL Fault	61
D. Fault Current Suppression and FRT for 1LG Fault	69
E. Index Based Comparison	76
F. Harmonic Study	77
G. Implementation Feasibility	79
H. Cost Effectiveness of the Proposed Approach	79
VIII Conclusion	81
A. Contributions from the Research	81
IX Future Work	83
References	84

LIST OF TABLES

Table	Page
1. Regional distribution of the global installed wind power capacity (MW) by 2012	3
2. Comparison of the Horizontal axis and the Vertical axis wind turbine	19
3. Onshore and offshore wind turbine comparison	22
4. Relative advantage and disadvantages of the FSWT and the VSWT	24
5. Up-wind and Down-wind turbine comparison	24
6. Relative comparison of the stall and the pitch control	29
7. Relative comparison of the wind generators used in WECS	32
8. Rating comparison of the power electronic components	33
9. Wind turbine data	40
10. Wind generator parameters	44
11. Values of the indices for performance comparison for 3LG fault	77
12. Values of the indices for performance comparison for LL fault	77
13. Values of the indices for performance comparison for 1LG fault	77
14. THD comparison	78

LIST OF FIGURES

Figure	Page
1. Oil price: inflation adjusted to 2007	1
2. Total world energy consumption by source (2011)	3
3. Global cumulative installed WECS capacity from 1996-2013	3
4. Market forecast for wind energy	4
5. Wind speed at different wind turbines of a farm and wind farm active power output	5
6. Low voltage ride-through standard set by FERC, U.S	7
7. Flow diagram of wind energy conversion system	11
8. Typical wind turbine power output with steady wind speed	12
9. Wind turbine	13
10. Turbine cross section	14
11. Wind turbine size: past, present and future	15
12. System level drive train technologies	16
13. Vertical axis wind turbine	18
14. Horizontal axis wind turbine	19
15. Onshore wind turbine	21
16. Offshore wind turbine	21
17. (a) Up-wind (b) Down-wind turbine	25
18. Up-wind and Down-wind hybrid Twin rotor turbine	25
19. Six mass drive train model	26
20. Three mass drive train model	27

21. Two mass drive train model	28
22. One-mass or lumped model	28
23. Typical power curves for a fixed speed, stall controlled (dashed) and variable speed, pitch controlled (solid) wind turbines	30
24. Vertical furling control	31
25. Generators used in the WECS	31
26. Types of self-commutated power converters for wind turbines: (a) a current source converter and (b) a voltage source converter	34
27. Full scale converter WECS	36
28. Partially rated converter WECS	36
29. Frequency converters	37
30. C_p - λ curves for different blade pitch angles (used in FSWT)	39
31. Arbitrary reference frame equivalent d-axis model of 3 phase symmetrical induction machine based wind generator	42
32. Arbitrary reference frame equivalent q-axis model of 3 phase symmetrical induction machine based wind generator	42
33. Detailed test system model	44
34. (a) Induction machine based wind generator equivalent and (b) simplified circuit. (c) Equivalent system diagram after fault	44
35. Per phase configuration of modified BFCL.	45
36. Matlab implementation of per phase modified BFCL	46
37. BFCL controller	48
38. Per phase BFCL controller implementation in MATLAB	49

39. Per phase SDBR topology	51
40. MATLAB implementation of SDBR	52
41. Per phase SDBR controller implementation in MATLAB	53
42. Fault current from line to ground in faulted line for 3LG fault.	55
43. Current at PCC for 3LG fault	56
44. Active power consumed in BFCL and SDBR for 3LG fault	56
45. Voltage at PCC for 3LG fault	57
46. Wind generator terminal voltage for 3LG fault	58
47. Wind generator speed response for 3LG fault.	59
48. Wind generator electrical torque for 3LG fault.	60
49. Wind generator active power output at PCC for 3LG fault.	60
50. Wind generator reactive power output at PCC for 3LG fault.	61
51. Fault current for LL fault.	62
52. Current at PCC for LL fault	63
53. Voltage at PCC for LL fault	63
54. Per phase voltage waveform at PCC for LL fault	64
55. Wind generator terminal voltage for LL fault	65
56. Wind generator speed for LL fault.	66
57. Wind generator electrical torque for LL fault.	66
58. Wind generator active power output at PCC for LL fault.	68
59. Wind generator reactive power output at PCC for LL fault.	68
60. Fault current from line to ground in faulted line for 1LG fault.	69
61. Current at PCC for 1LG fault	70

62. Voltage at PCC for 1LG fault	71
63. Wind generator terminal voltage for 1LG fault	71
64. Per phase voltage waveform at PCC for 1LG fault	72
65. Wind generator speed for 1LG fault.	73
66. Wind generator electrical torque for 1LG fault.	74
67. Wind generator active power output at PCC for 1LG fault.	75
68. Wind generator reactive power output at PCC for 1LG fault.	75

LIST OF ABBREVIATIONS

1LG	-	Single-Line-to-Ground
2LG	-	Double-Line-to-Ground
3LG	-	Three-Line-to-Ground
BFCL	-	Bridge-Type Fault Current Limiter
BJT	-	Bipolar Junction Transistor
CSC	-	Current Source Converter
DFIG	-	Doubly Fed Induction Generator
DVR	-	Dynamic Voltage Restorer
FRT	-	Fault Ride-Through
FSWT	-	Fixed Speed Wind Turbine
GTO	-	Gate Turn-Off Thyristor
GW	-	Giga Watt
HAWT	-	Horizontal Axis Wind Turbine
HTS	-	High Temperature Superconducting
IGBT	-	Insulated-Gate Bipolar Transistor
IGCT	-	Integrated Gate-Commutated Thyristor
LL	-	Line-to-Line
LVRT	-	Low Voltage Ride Through
MERS	-	Magnetic Energy Recovery Switch
MOSFET	-	Metal–Oxide–Semiconductor Field-Effect Transistor
MW	-	Mega Watt

PCC	-	Point of Common Coupling
PMSG	-	Permanent Magnet Synchronous Generator
SCADA	-	Supervisory Control and Data Acquisition
SCIG	-	Squirrel Cage Induction Generators
SDBR	-	Series Dynamic Braking Resistor
SFCL	-	Superconducting Fault Current Limiter
SR	-	Switched Reluctance
STATCOM	-	Static Synchronous Compensator
SVC	-	Static Var Compensator
THD	-	Total Harmonic Distortion
TSC	-	Thyristor Switched Capacitor
VAWT	-	Vertical Axis Wind Turbine
VSC	-	Voltage Source Converter
VSWT	-	Variable Speed Wind Turbine
WECS	-	Wind Energy Conversion Systems
WFSG	-	Wound Field Synchronous Generator

CHAPTER I

INTRODUCTION

Wind is one of the most important renewable resources like sunlight, water etc. Sailboat and sailing ships were propelled utilizing wind power thousands of years ago. In the middle age, people used wind mill for irrigation and grinding wheat to make flour [1]. It was the end of nineteenth century when energy contained in wind flow was exploited to generate electricity by Scottish Professor James Blyth [2]. Since then, wind energy technology was having slow advancement and improvement until the oil price hike in the 70's as seen in Figure 1. This price hike and fluctuation of oil price made the policy makers to think of alternative source of energy. As wind is a good potential source of renewable energy, a great amount of research and development effort has been given for the improvement of wind energy technology that continues till present days. The research effort was even more accelerated and much emphasis is given on wind energy due to the

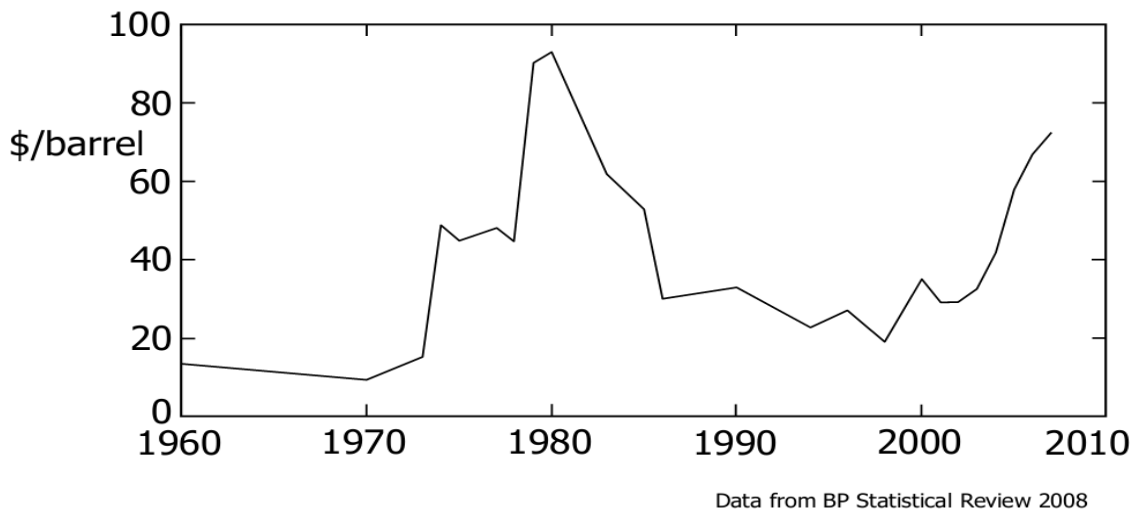


Figure 1. Oil price: inflation adjusted to 2007

fact that fossil fuel is limited in reserve and someday, they will be finished. Policy makers are also moved by the effect of the global warming resulting from burning fossil fuel. Reduction of carbon emission is an important concern now, and low tax on low carbon technology has made renewable energy popular than ever. All these factors have paved the way for wind energy conversion systems (WECS) to travel from professor Blyth's era towards present day to be a strong contender of world's energy crisis solution among the options available. WECS continues to get more and more importance and attention all over the world and contributes a portion of renewable energy produced globally [3].

A. Global Wind Energy Status

Wind energy has gained much popularity as a renewable energy source all over the world. It has its footprint in all regions of the world as evident from the statistics of Table 1.

Apart from bio sources and hydropower, wind energy is the most power delivering renewable source as shown by Figure 2. In recent times, starting from 1996 to 2013 global cumulative installed wind capacity has become 319 GW from 6.1 GW as shown in Figure 3.

B. Wind Energy in Future

It is apparent that the wind energy industry is growing very rapidly. It is expected by the experts that it'll supply about 10% of worlds electricity generation by year 2020 [1]. Market forecast for the year 2013-2017 by GWEC also supports this fact as shown in Figure 4 [4].

Table 1. Regional distribution of the global installed wind power capacity (MW) by 2012

Region	Wind Power Capacity (MW)
Africa and Middle East	1135
Asia	97570
Europe	109581
Latin America and Caribbean	3505
North America	67576
Pacific Region	3219

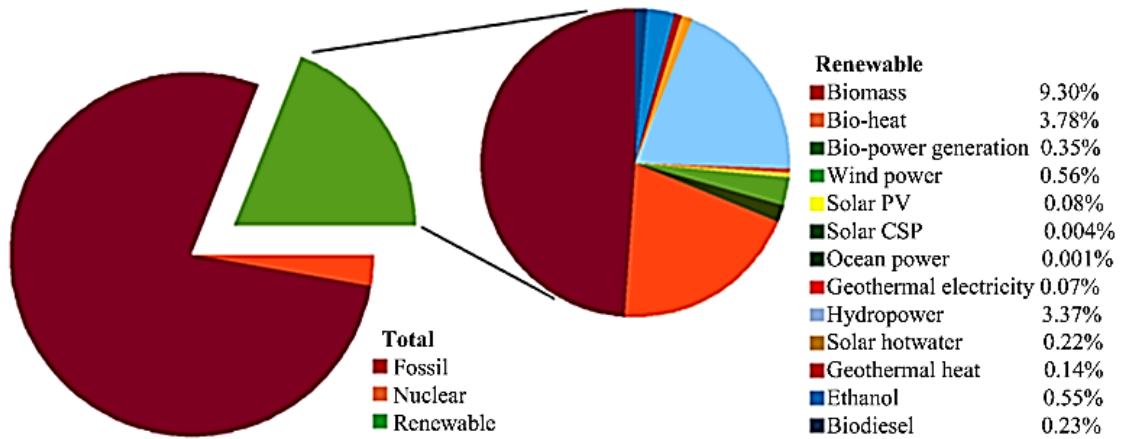


Figure 2. Total world energy consumption by source (2011) [3]

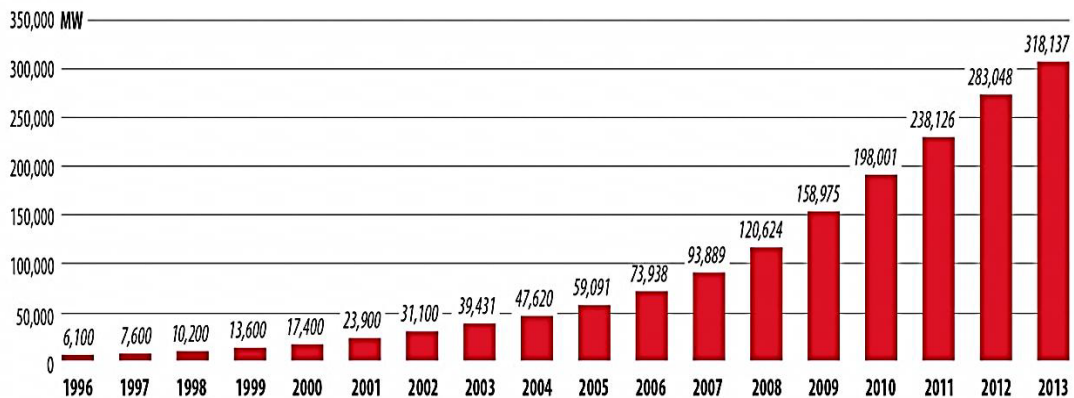


Figure 3. Global cumulative installed WECS capacity from 1996-2013[4]

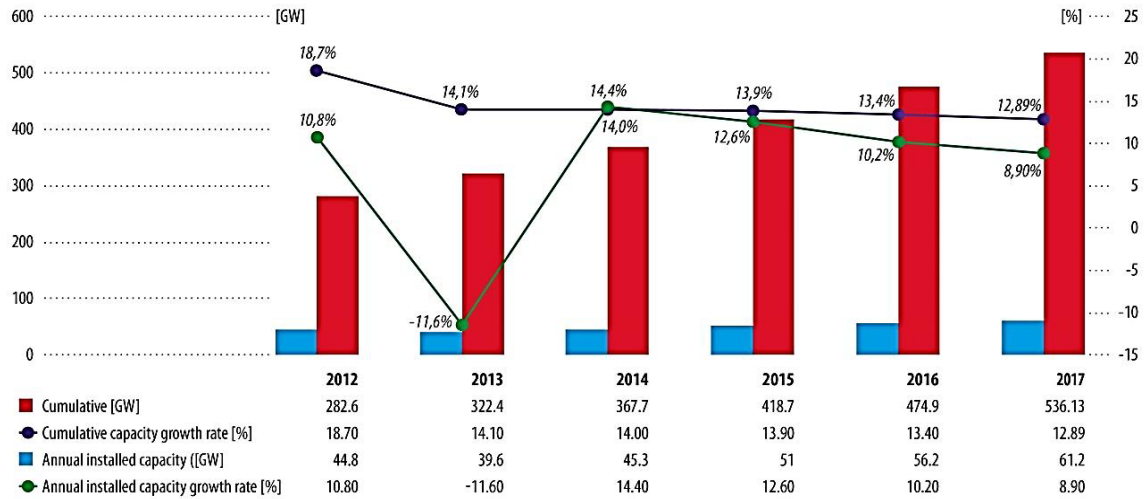


Figure 4. Market forecast for wind energy

C. Background and Literature Review

Wind energy is the most prominent alternative energy source for producing electric power due to its zero fuel cost, no carbon emission, cleanliness and renewable nature [5]. To supply electric power from WECS to the consumers, integration of wind energy sources into the existing grid is needed. To realize this, it is essential that the wind energy sources behave like a conventional energy sources. But the wind speed is not constant; rather it's a function of geographic location, air temperature, altitude from sea level etc. An example of wind speed profile at different turbines of a wind farm is shown in Figure 5. Fluctuating wind speed consequently causes fluctuation in produced power, which is evident from the wind farm active power output of the farm in Figure 5.

To solve the issue of wind farm output power fluctuation with variable wind speed, use of superconducting magnetic energy storage (SMES) [5]–[7], capacitor energy storage (CAES) [8], flywheel energy storage (FES)[9] etc., are proposed in literature. Also pumped hydro energy storage (PHES), compressed air energy storage (CAES), fuel

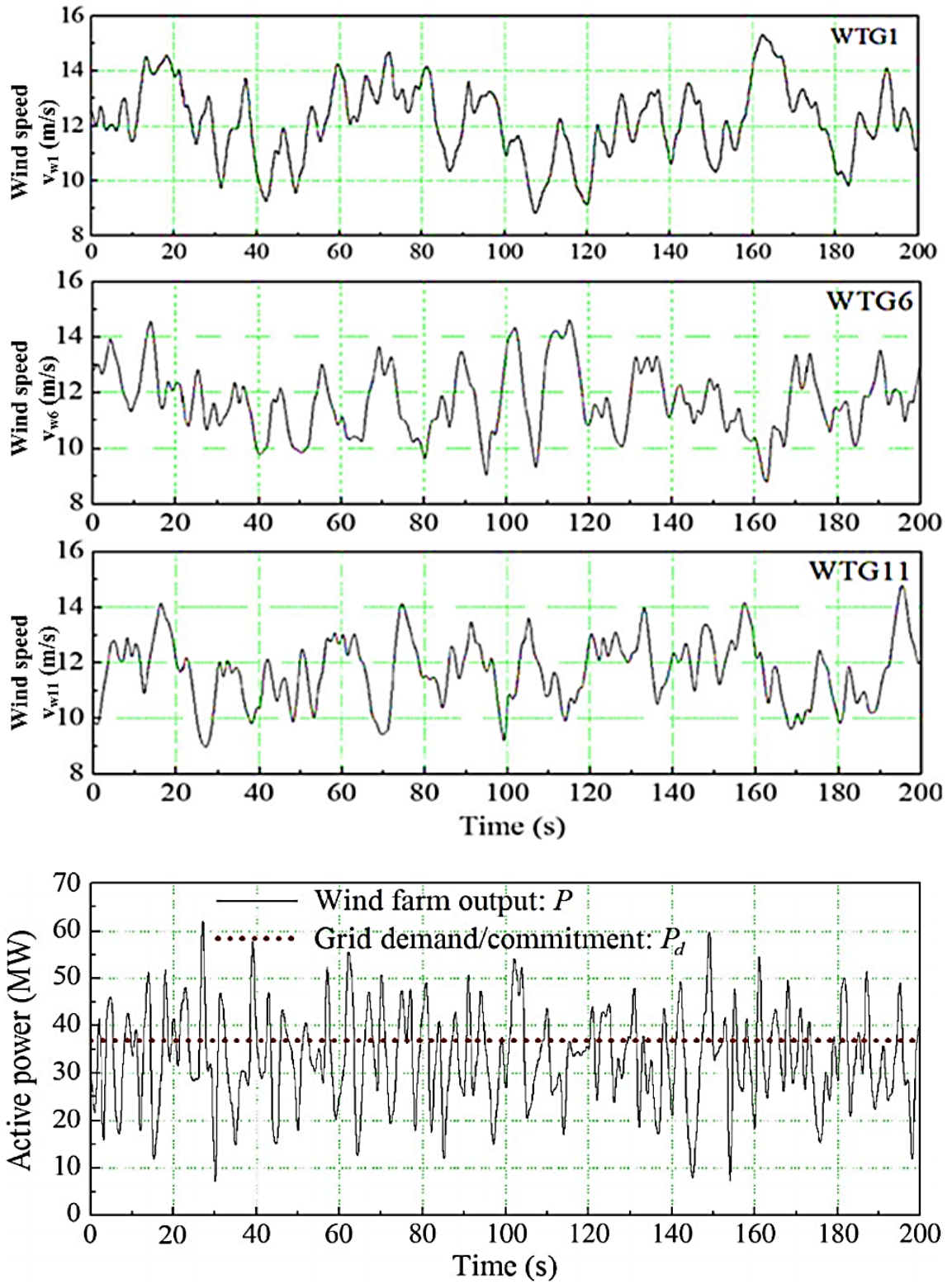


Figure 5. Wind speed at different wind turbines of a farm and wind farm active power output

cell energy storage are potential candidates to tackle this problem[10]. Apart from the fluctuating wind power output, there are issues with the grid integration of wind generator and their sustained operation. This thesis focuses on an important aspect of grid integration of wind generator which is the fault ride through capability.

One of the major problems in the conventional grid is fault (accidental connection to ground). The existing grid elements are designed and engineered to handle different fault scenario. The WECS are newer elements and by nature they are vulnerable to faults. Extensive investigation regarding interaction between wind turbines and power grid has been carried out in recent years [11], [12]. Two main problems with WECS during the fault condition are decrement in fault ride-through (FRT) capability and increase in short-circuit current level. As the wind turbines are sensitive to fault, traditionally they were disconnected from grid to isolate and protect them. This technique had no negative effect on power system because the amount of wind integration used to be small. But at present days, there are some countries like Denmark and United kingdom, receive a significant portion of their electrical power from wind energy [5]. Modern day large-output wind turbines, having capacity of 1 MW and above, are normally required to include auxiliary systems that allow them to operate through fault event, and thereby "ride through" the low voltage [13]. If wind farms are disconnected at fault in a system where wind energy shares a significant portion, nearby generators and rest of the system might get affected in a chain reaction manner. So these WECS are needed to be connected to grid and continue operation at faulted situation and may need provide reactive power support to help rest of the system recover from fault. This event of WECS remaining operational and connected to grid at fault is commonly known as FRT. It is also sometimes termed as low voltage ride through (LVRT). Also to interface the wind generators into the existing grid, grid

codes [14] specified for many countries must be satisfied. Special arrangement is required to abide by the grid code. Grid code to integrate wind energy into USA power grid is given in Figure 6.

As more and more WECS are connected to the grid, fault current level of the grid increases. This causes the circuit breaker interruption capacity to surpass the rated current and instantaneous voltage sag at the fault event. However, circuit breakers sometimes become incapable of handling the extreme level of fault current, so they fail to operate. Handling the increasing fault currents often involves costly replacement of substation components or alteration of coordinated control resulting in decreased operational flexibility and lower reliability. This replacement might be ineffective for some operating scenarios and the FRT and fault current suppression may not be ensured.

To improve the FRT of the WECS, both parallel and series types of compensation devices are used. Static synchronous compensator (STATCOM) [5], [15], thyristor switched capacitor (TSC) [16], static var compensator (SVC) [15], SMES [6], [17], [18] are used as parallel options, and series dynamic braking resistor (SDBR) [19], dynamic

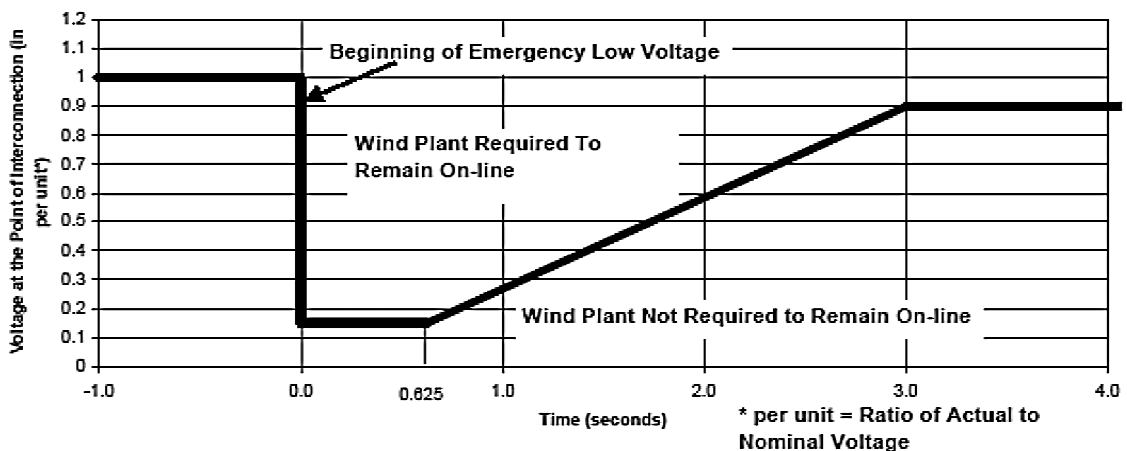


Figure 6. Low voltage ride-through standard set by FERC, U.S [20]

voltage restorer (DVR) [21], [22], magnetic energy recovery switch (MERS) [23], superconducting fault current limiter(SFCL) [24], transformer coupled bridge-type fault current limiter (BFCL) [25], are among the series options. Besides these electrical auxiliary device solutions, there is another solution which is a mechanical solution named as pitch control. This also has the ability to make the WECS capable of achieving FRT [26].

D. Motivation

These days, development of minimum cost, high output power and cheaper wind energy conversion systems (WECS) is the hot research topic around the world. At present, variable speed wind turbines (VSWT) are mostly used due to their higher output power and efficiency, improved power quality, reduced mechanical stress on turbine and independent control of active and reactive power etc. [5]. But, over the past years, fixed speed wind turbine (FSWT) systems were installed in large scale across the globe. FSWT exploits squirrel cage induction generators (SCIG) directly connected to the power grid.

As the SCIGs are robust in nature, wind parks facilitated by them have a lifetime over 20 years [27], and hence it is still important to study integration issues of the fixed-speed WECS into the existing power system.

The STATCOM requires power electronics converter and complex control strategy resulting in complexity into the systems, whereas the TSC and the SVC suffer from poor performance issue. SMES and SFCL perform better [24] but it is not economically feasible to implement as it requires cryogenic cooling facility for superconducting operation and incurs high installation and operation cost. BFCL configuration used in [24], [25] requires additional converter unit with a 12 lid coupling transformer which makes is complex and hardware consuming. Also there is extra line loss incurred by the

transformer as it is connected in series with the line. The DVR shows promising performance but they also have controller complexity and higher number of required electronic components. The SDBR gives slow transient response and lesser oscillating torque damping.

The bridge type fault current limiter (BFCL) is a new technique that has promising applications in fault ride through of the WECS [24], [25] and dynamic performance improvement of power systems [28], [29]. So, it is worth investigating their performance on a FSWT systems based on the SCIG with some modification.

E. Novelty

With such background, this work proposes a new modified configuration of the BFCL, which is different from the one used in [13]-[16], to achieve the FRT of the fixed speed wind generator system. Here it is important to note that the dc reactor placed within the bridge of the proposed BFCL limits a sudden rise of fault current instantaneously. Thus sudden voltage drop at machine terminal is prevented during fault and hence it provides improved transient behavior. This unique feature of the BFCL makes it favorable over the other series FRT measures. A shunt bypass path helps maintain voltage at the point of common coupling (PCC) and machine terminal. In this way it helps to moderate that portion of electrical torque which is responsible for instability and also increases the active power demand to machine during fault. Unlike [24], [25], the shunt path of the BFCL used in this work, consists of only resistor. The inductor is omitted because it discharges stored energy when the shunt path is disconnected. It makes fault performance worse.

The SDBR is a popular and low cost solution. This has applications in power systems [30]–[33]. Its principle of operation is similar to the BFCL and both of them are the series

type solution. In order to see how much effective the proposed BFCL is, in improving the FRT of the wind generator, its performance is compared with that of the SDBR. Along with simulation, an index based comparison is carried out to give a clear insight.

Simulations were carried out using Matlab/Simulink software. In order to demonstrate the effectiveness of the proposed approach, a temporary three-line-to-ground (3LG), a line-to-line (LL) and single-line-to-ground (1LG) faults were applied at one of the lines of the considered test wind generator system.

F. Thesis Organization

In chapter II an overview on the WECS is given. Modeling of the wind turbine and wind generator is described in chapter III. The test system model is illustrated in chapter IV. The BFCL and SDBR configuration, operation, design and control are explained in chapters V and VI, respectively. Simulation results are discussed in chapter VII. Chapter VIII wraps up the findings in this work in a conclusion, and finally chapter IX provides some future research directions.

CHAPTER II

WIND ENERGY CONVERSION SYSTEM (WECS) OVERVIEW

A wind energy conversion system converts the kinetic energy in the wind into electrical energy. Kinetic energy is received by some arrangement, for example turbine blade, which is used to create a rotational motion. This converts the kinetic energy in wind motion into mechanical energy. The rotational mechanical energy in turbines is used to rotate the rotor shaft of a wind generator. The generator takes the mechanical energy and then converts it into electrical energy. The generated electrical energy is then fed to load or electrical grid. A high level diagram of this conversion process is shown in Figure 7.

As we know that many renewable sources are intermittent, the wind speed varies over time. Turbines are designed in a way that they require a minimum wind speed to start electricity production. This is called cut in wind speed and it varies in the range of 3 to 5m/s for different wind turbines. As the wind speed goes up, output energy increases in non-linear manner. The speed, at which the nominal power output of the turbine is achieved, is called nominal wind speed. Depending on rotor and blade design of turbines, nominal speed varies between 11 m/s and 16 m/s [34]. If the wind speed goes beyond the nominal speed, then the output power is kept constant at nominal output power by controlling turbine efficiency through some mechanical arrangement like stall control,



Figure 7. Flow diagram of wind energy conversion system

pitch control or active stall control. There is a maximum threshold of wind speed, beyond which operation of a wind turbine is risky enough to cause mechanical damage. This is called cut out wind speed. When cut out wind speed is exceeded, wind turbine is taken out of operation. Depending on whether the wind turbine is designed to operate at low or high wind speed, the cut out wind speed is ranged between 17 and 30 m/s. Figure 8 shows the relation of wind speed with the electrical output power of a typical wind turbine.

In the following subsections, an overview on the WECS is given.

A. Wind Turbine Components.

Wind turbine is the device that does the wind energy conversion as a whole. The construction and design of a wind turbine involves electrical, mechanical and civil engineering. Figure 9 and 10 show the components of a typical turbine,

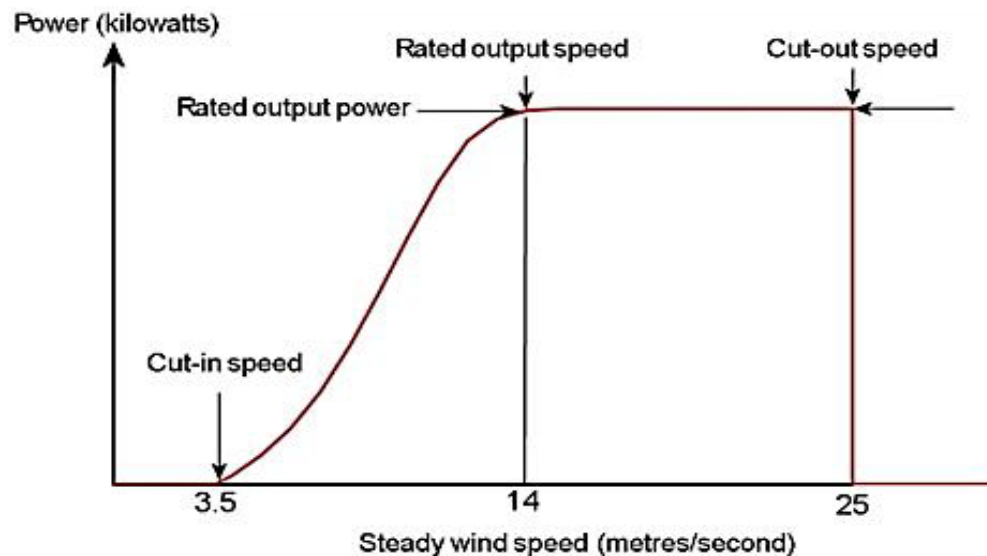


Figure 8. Typical wind turbine power output with steady wind speed [35]

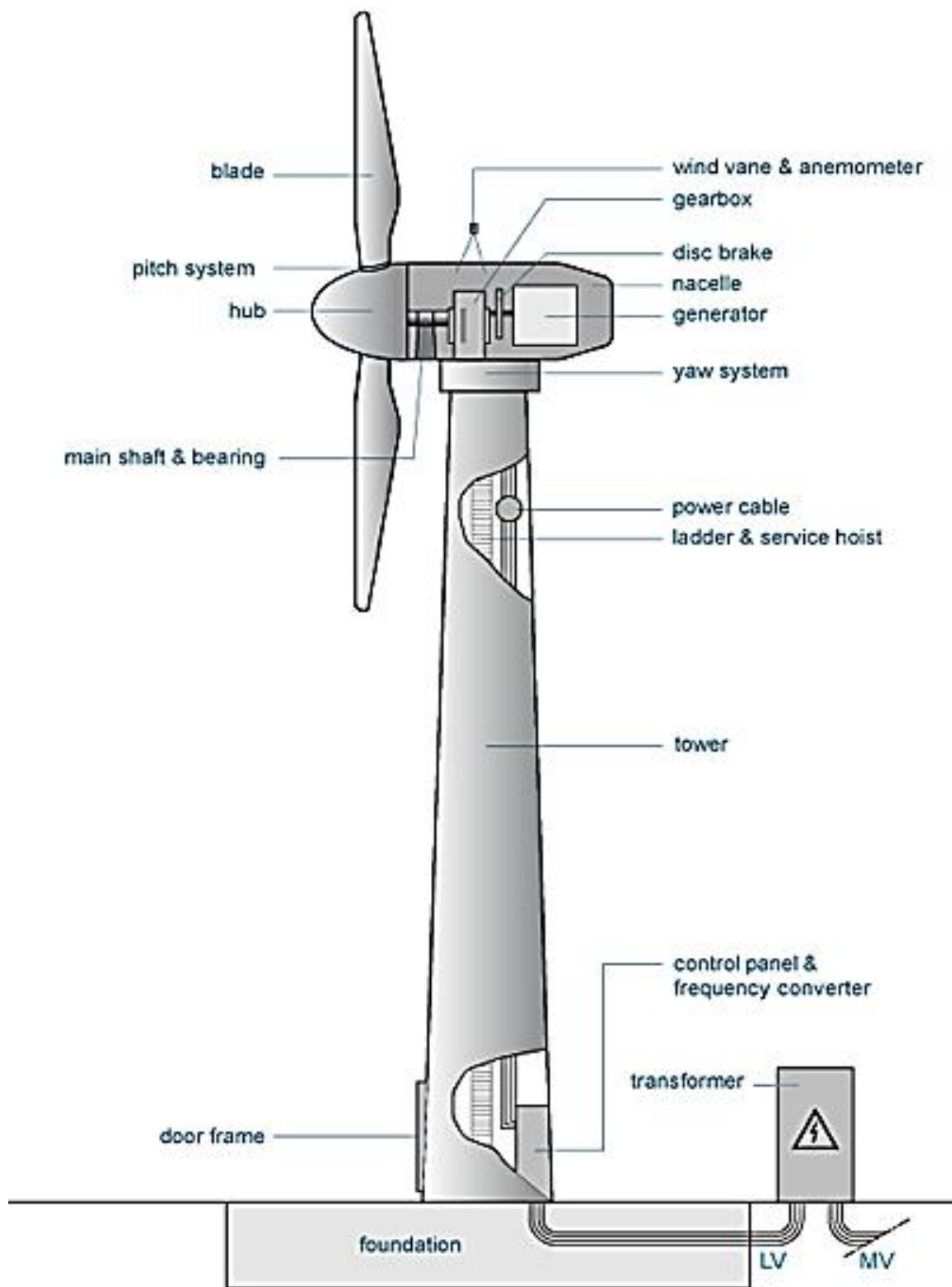


Figure 9. Wind turbine [36]

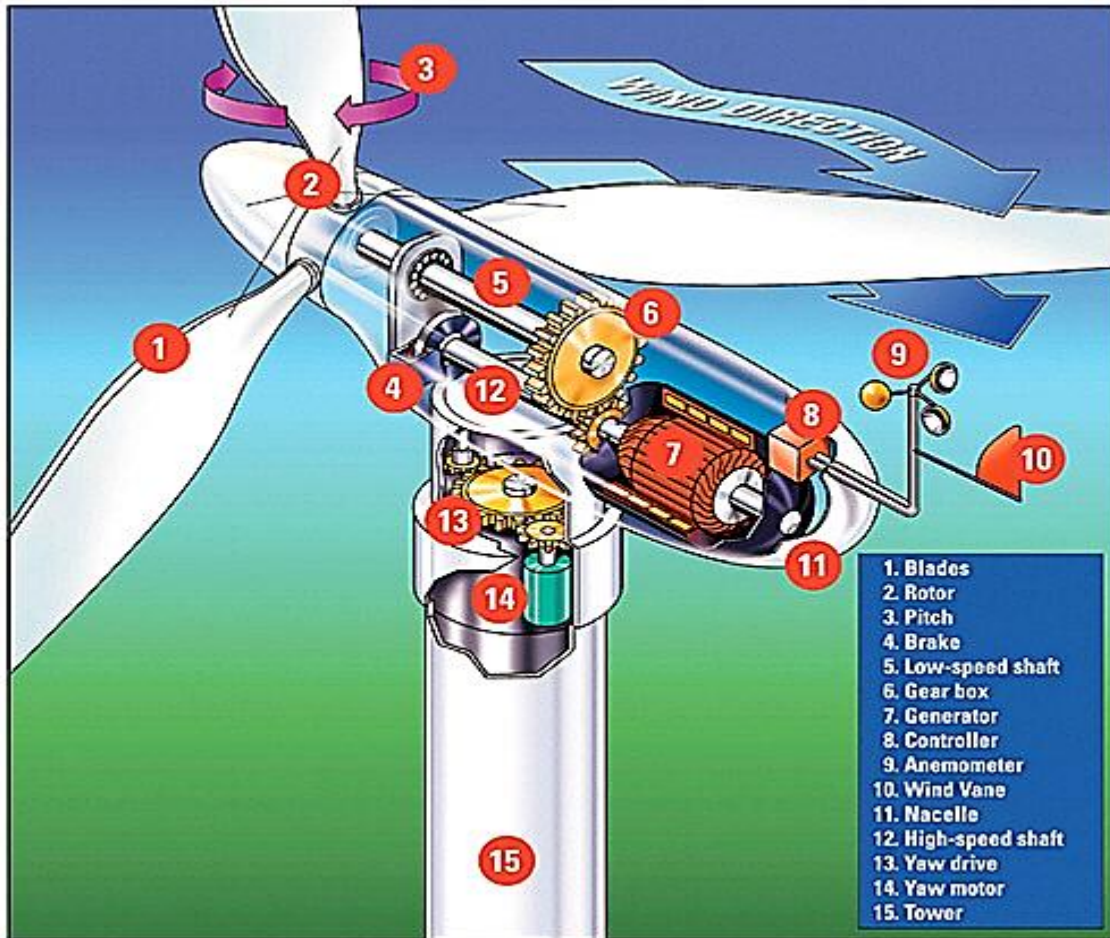


Figure 10. Turbine cross section [37]

Turbine blades: Blades are the airfoils in the modern day wind turbines that actually receive the kinetic energy. Therefore blade diameter is a clear indicator of a wind turbine power production capacity. Also the design and material used in it play the key role. Fiberglass reinforced with polyester and wood epoxy are popular material for blade construction. Blade rotation speed reduces with the increase of blade diameter and typically ranges from 3-30 rpm which can be fixed or variable speed. the tendency of placing wind turbines to offshore is also increasing with increase in blade diameter as shown in Figure 11 [36].

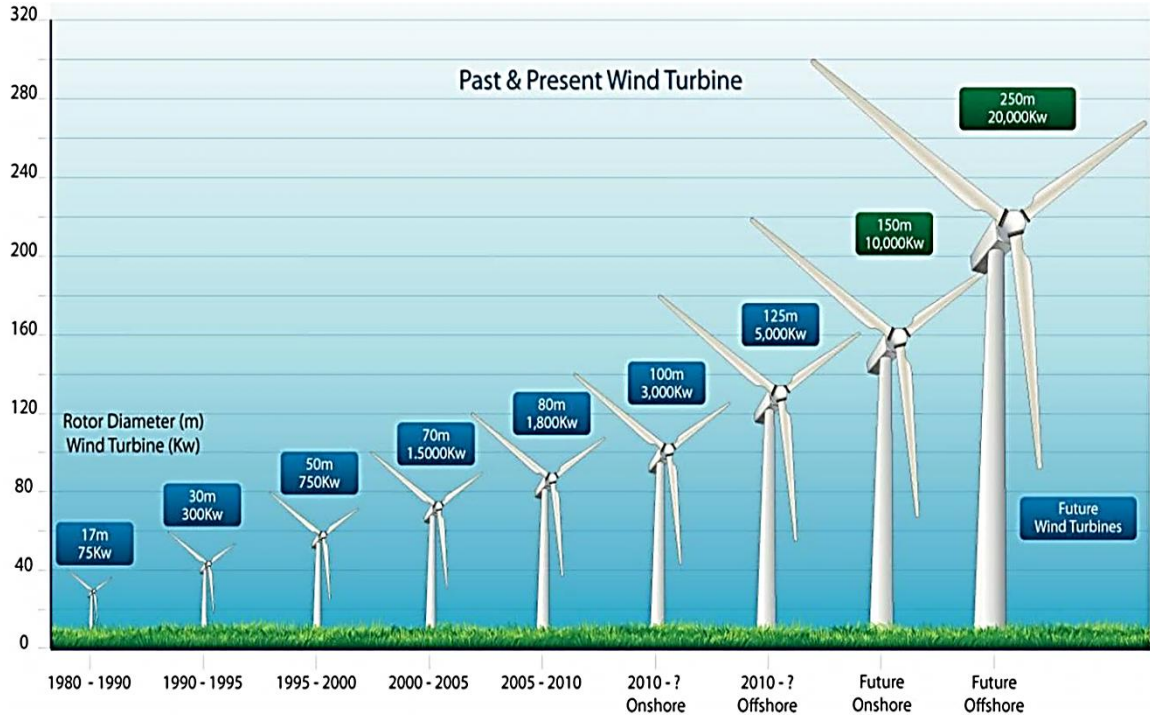


Figure 11. Wind turbine size: past, present and future [38].

Turbine hub: Turbine hub is the point where all the blades are connected. It also carries the pitch control system.

Shaft: Turbine hub is connected to the gear box or the direct drive system through a mechanical shaft.

Gear box: This is the arrangement that converts the low blade rotation speed into high generator rotor speed. It also actively takes part in maintaining desired speed of the generator rotor shaft.

Direct drive: As the gear box system is costly and requires frequent maintenance, some manufacturers directly couples the shaft into the generator rotor. Drive train types are shown in Figure 12.

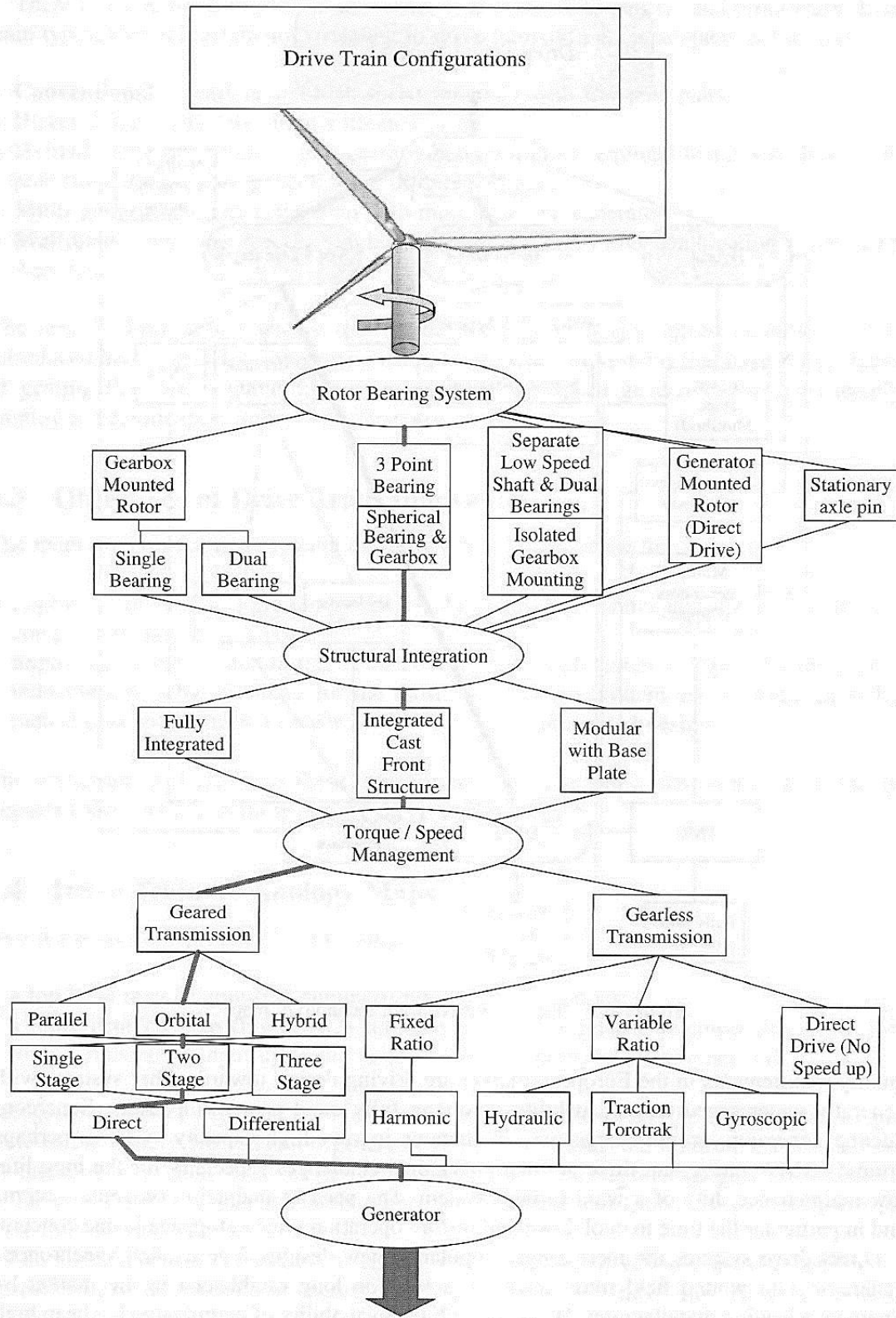


Figure 12. System level drive train technologies [39]

Generator: It is the electrical machine to convert the mechanical energy into electrical energy. Depending on operating criteria, their type varies.

Pitch control: To control the efficiency of the turbine, blades are aligned at desired angle with the wind direction. This is achieved by the pitch control and it is located in the turbine hub.

Yaw system: To align the blade rotation plane in perpendicular with the wind direction yaw system is used. This system interfaces the tower with the nacelle.

Nacelle: The covered thing that is placed on top of the tower is the nacelle and it contains gearbox, shaft, generator, power electronic equipment's, switchgear, wind flow direction and speed detection sensors etc.

Transformer: Normally electricity is generated at low voltage. To transmit the generated electricity, stepping up of the voltage is necessary. So the turbines are equipped with transformers that are typically placed on ground very close to tower base.

Tower: Tower is the support for nacelle and it gives the turbine strength. Power lines go through the tower to connect the generator to the transformer. Ladder and service hoist are also placed inside the tower. Now-a-days, there are some airborne wind turbines which don't need stiff and strong tower.

Foundation: Tower is attached to a solid foundation whether it is placed onshore or offshore.

B. Wind Turbine Types

The wind turbines are classified depending on various aspects like axis of rotation, location of installation, output power scale, generator rotor speed, power electronic converter rating, generator type used. They are described as follows.

1) Axis of Rotation

The vertical axis wind turbine (VAWT) and horizontal axis wind turbine (HAWT) are the two wind turbine types based on axis of rotation [5]. A brief description follows.

Vertical axis wind turbine (VAWT): The generator shaft is positioned vertically with the blades rotating around it. They are normally of small height. An example is given in Figure 13.

VAWT can be of two types namely a) drag type and b) lift type.

Horizontal axis wind turbine (HAWT): In this type of turbine, the generator shaft is positioned parallel to the ground and the blades are positioned on top of a long tower. The HAWT is taller and this type is popular for its high output power. A HAWT is shown in Figure 14.

A comparison between HAWT and VAWT is given in tabular form in Table 2.



Figure 13. Vertical axis wind turbine [5]



Figure 14. Horizontal axis wind turbine [40]

Table 2. Comparison of the Horizontal axis and the Vertical axis wind turbine [41]

	Horizontal axis	Vertical axis
Power generation efficiency	50%-60%	Above 70%
Electromagnetic interference	Yes	No
Steering mechanism of wind	Yes	No
Gear box	For greater than 10 kW	No
Blade rotation space	Quite large	Quite small
Wind resistance capacity	Weak	Strong (can resist typhoon upto class 14)
Noise	5-60 dB	0-10 dB
Starting wind speed	High (2-5m/s)	Low(1.5-3m/s)
Ground projection effect on human being	Dizziness	No effect
Failure rate	High	Low
Maintenance	Complicated	Convenient
Rotating speed	High	Low
Effect on birds	Great	Small
Cable stranding problem	Yes	No
Power curve	Depressed	Full

2) *Installation Location*

Traditionally, the wind turbines were installed on land. But in 1991, the first wind turbine was installed on the shallow sea near coast [42]. They are termed as offshore wind turbine. To distinguish an offshore wind turbine, wind turbines placed on land are termed as onshore wind turbine.

Onshore wind turbine: This is the old concept of wind turbine placement. They provide good performance at low installation along with low maintenance cost but gives low efficiency. Figure 15 shows onshore wind turbine.

Offshore wind turbine: Offshore turbines as in Figure 16, give higher efficiency as the wind speed at offshore location is higher and more uniform. They are gaining popularity and large capacity wind turbines that are built at present days are offshore type.

Airborne wind turbine: There is a new type of wind turbine which is placed in air floating like kites. These types are still in research and their prototype are showing huge potential [43].

Advantages and disadvantages of onshore and offshore wind turbine are given in Table 3.

3) *Output Power Scale*

Day by day output electrical power capacity of the wind turbine is increasing. According to the output power capacity, they can be categorized into different classes [44]. Purpose at hand defines the power scale to be selected by the user. Small and medium scale turbines are utilized in remote standalone system and large scales wind turbines are connected to microgrids and power grids.

Small scale wind turbine: They can operate at fairly low annual wind speed ranging from 2.5 to 4 m/s with fairly low capacity of 0.025kW to 10kW.



Figure 15. Onshore wind turbine [45]



Figure 16. Offshore wind turbine

Table 3. Onshore and offshore wind turbine comparison

	Onshore wind turbine	Offshore wind turbine
Advantages	<ul style="list-style-type: none"> -Cheaper foundations; -Cheaper integration with the electrical-grid network; -Cheaper installation and access during the construction phase -Cheaper and easier access for operation and maintenance. 	<ul style="list-style-type: none"> -Higher and more constant wind speeds -Higher efficiencies -Low pay-back time -Higher production capacity
Disadvantages	<ul style="list-style-type: none"> -Negative visual impact -Noise; -Restrictions associated with obstructions (buildings, mountains, etc.), land-use disputes -Limited availability of lands. -Harm to birds 	<ul style="list-style-type: none"> -Higher installation cost -Effect on many living sea organisms

Medium scale wind turbine: They give output power from 10kW to 100kW and operate fairly at an annual wind speed of 4 to 5m/s.

Large scale wind turbine: Any wind turbine with output power capacity larger than 100kW lies in this range and they need average annual speed over 5 m/s.

4) *Rotational Speed*

According to the rotational speed, there are two types of wind generator systems: (1) fixed speed; and (2) variable speed. The primitive wind turbines were fixed speed type but for the last decade variable speed types are mostly used for new installations.

Fixed speed: Induction machines are used as fixed speed wind generators. This system is also referred to as the Danish concept. In the start-up sequence, the rotor may be held stopped and as the brakes are released, rotor shaft would be accelerated by the wind until the desired fixed speed is reached. At this instant, grid connection would be made and then the grid (through the generator) will hold the constant speed. When the wind speed is increased beyond the rated power generation level, power production will be regulated

by stall or by pitching the blades to match with the grid frequency. Speed variation is very low, typically 1~2% of the nominal speed. A soft starter is used to reduce the startup inrush current. A reactive power compensator (i. e. fixed capacitor) is also needed to reduce the reactive power demand of a fixed speed wind generator.

Variable speed: In this type of generator, blade speed is matched with wind speed and generated power is conditioned by power electronic converters. The rotor could be connected to the grid at low speeds in very light winds and would speed up in proportion to wind speed. As rated power production is reached, the turbine shaft reverts to nearly constant speed operation. To accomplish this, blades are pitched at appropriate angle. Wound field synchronous generator (WFSG), permanent magnet synchronous generator (PMSG) and doubly fed induction generator (DFIG) are the most commonly used variable speed wind turbines.

Their relative advantage and disadvantages are given in Table 4.

5) Axis Orientation and Hub

If axis orientation and hub is considered then there come two variants of turbine. There is one where the wind hits the blades first called (1) Up-wind turbine and another one where the wind hits the tower first and then the blades called (2) Down-wind. Their relative comparison is presented in Table 5.

Figure 17 shows the Up-wind and Down-wind type wind turbine. To get the full advantage of both of the types, a twin rotor wind turbine is proposed as shown in Figure 18.

Table 4. Relative advantage and disadvantages of the FSWT and the VSWT

	Fixed speed wind turbine	Variable speed wind turbine
Advantages	<ul style="list-style-type: none"> -Simple, robust and reliable -Proven technology -Low cost of electrical parts -Low maintenance -Higher lifetime 	<ul style="list-style-type: none"> -Higher energy capture -Improved power quality -Reduced mechanical stress -Higher efficiency -Higher output power capacity -Complete and separate control of reactive and active power -Gear system can be avoided
Disadvantages	<ul style="list-style-type: none"> -Uncontrollable reactive power consumption -High mechanical stress -Limited power quality control -Low efficiency - Fluctuation of wind speed is transmitted to grid -Lower stability -Lower efficiency -Lower Output power capacity 	<ul style="list-style-type: none"> -Costly -Higher maintenance required -Equipment consuming -Power electronic converter required

Table 5. Up-wind and Down-wind turbine comparison

Up-wind	Down-wind
<ul style="list-style-type: none"> - It provides less variation in the power output. - Tower shadow effect is avoided. - A rigid hub is required. A fair separation of hub from the tower is necessary. Else, the bending blades may hit the tower. - This is the popular design for turbines in the MW- range mostly. 	<ul style="list-style-type: none"> - Yaw mechanism can be avoided if the nacelle is designed with a streamlined body that will make it aligned to the wind direction. - More flexible rotor is possible. Blades can bend at higher speed, releasing load off the tower. - Higher fluctuations in wind power, as blades are affected by the tower shadow. - Employed only in small wind turbines.



Figure 17. (a) Up-wind (b) Down-wind turbine [46]



Figure 18. Up-wind and Down-wind hybrid Twin rotor turbine [47]

C. Drive Train System

In literature, few types of models for the wind turbine drive train are available [48].

They are given below:

- Six-mass drive train model
- Three-mass drive train model
- Two-mass shaft model
- One-mass or lumped model

1) *Six-Mass Drive Train Model*

The basic six-mass drive train model is presented in Figure 19. This is the most detail system and it captures almost all the dynamics of the mechanical system. This model is suitable for elaborative studies where the turbine performance with wind speed variation is of importance. It consists of six inertias: the three blade inertias (J_{B1} , J_{B2} and J_{B3}), hub inertia J_H , gearbox inertia J_{GB} and generator inertia J_G . Other secondary drive train elements inertia like axes, disc brakes, etc. is lumped into them. Angular positions of the blades, hub, gearbox and generator are given by Θ_{B1} , Θ_{B2} , Θ_{B3} , Θ_H , Θ_{GB} and Θ_G respectively. ω_{B1} , ω_{B2} , ω_{B3} , ω_H , ω_{GB} and ω_G represent the rotational velocities of the blades, hub, gearbox and generator. The mutual damping between nearby masses is expressed by d_{HB1} , d_{HB2} , d_{HB3} , d_{HGB} and d_{GBG} . The elasticity between neighboring masses is expressed by the spring constants K_{HB1} , K_{HB2} , K_{HB3} , K_{HGB} and K_{GBG} . Individual masses cause some torque losses represented by D_{B1} , D_{B2} , D_{B3} , D_H , D_{GB} and D_G . The turbine torque is the sum of the individual blade torques T_{WT} . The generator torque is T_E and three individual aerodynamic torques T_{B1} , T_{B2} and T_{B3} are acting on the three blades. The aerodynamic torques acting on the hub and gearbox are assumed to be zero.

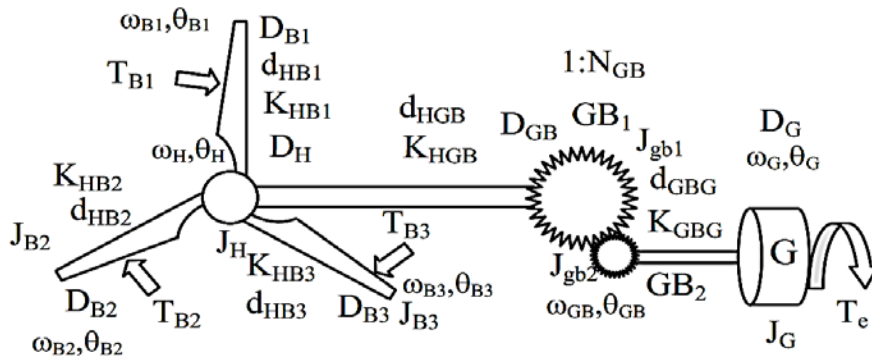


Figure 19. Six mass drive train model [49]

2) Three-Mass Drive Train Model

In three-mass drive train mode it is assumed for simplicity that the three-blade turbine has same weight. The turbine torque T_{WT} , is assumed as the sum of the torques on the three blades. So the turbine hub and blade mass can be lumped into a single mass and the six mass system is reduced to a three mass system as shown in Figure 20. Also the two separate masses of the gearbox can be thought of a single mass. This model is called transformed tree mass model as in Figure 20.

3) Two-Mass Shaft Model

The three-mass system can be converted into a two-mass system by adding the gearbox mass either with the turbine mass or the generator mass as shown in Figure 21. In this model the shaft has a uniform stiffness. Three mass or two mass drive train model is suitable for studies that investigate steady state and longtime performance of a turbine. The six mass system is very detail and hard to model. It takes long time to simulate a six mass system. It is reported that two or three mass model gives good result without loss of that much accuracy [48].

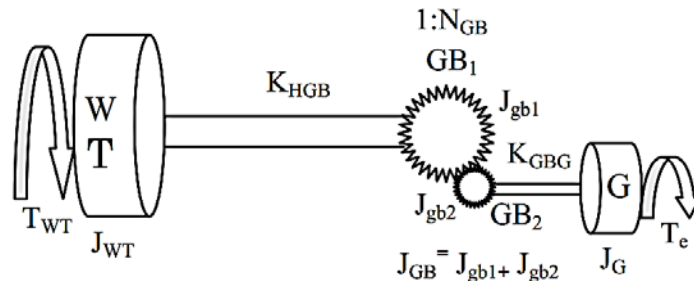


Figure 20. Three mass drive train model [50]

4) *One-Mass or Lumped Model*

The most simple of all drive train models is the one mass or lumped mass model as shown in Figure 22. Here all the masses are lumped into a single mass. This single mass system is suitable for transient stability studies where the time duration of interest is small, for example fault studies.

D. Speed and Torque Regulation of Wind Turbines

The turbine speed and torque control mechanism is a speed regulation technique for overspeed control as well as the rotors to be slowed down or stopped. Its purpose is to

- Make maintenance possible
- Reduce noise pollution

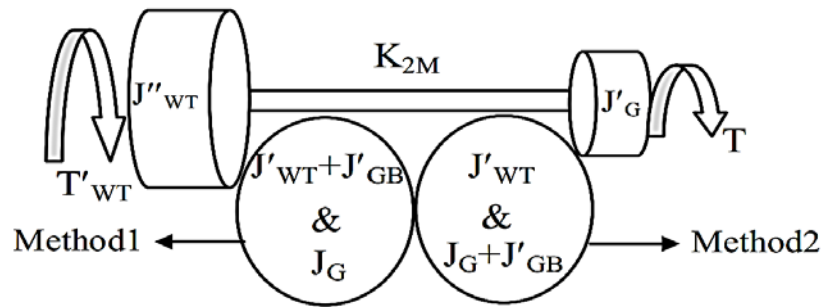


Figure 21. Two mass drive train model [49]

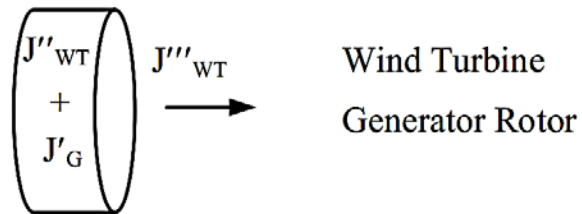
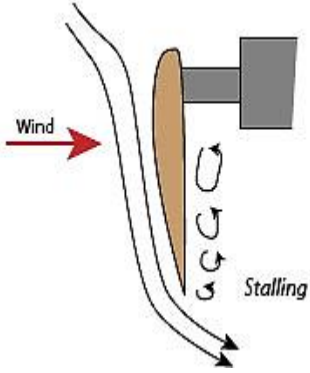
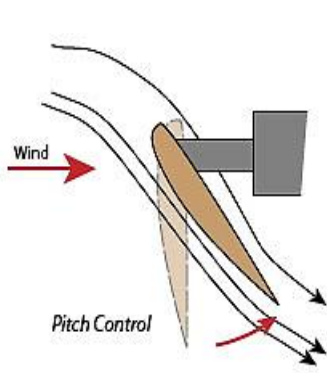


Figure 22. One-mass or lumped model [48]

- Tune aerodynamic efficiency
- Retain the generator with its torque and speed limits
- To keep the rotor and the tower within their mechanical strength limits.

There are three popular methods to do it. (1) Stall control, (2) Pitch control and (3) Furling [46]. Their functions, principles and relative comparison of stall and pitch are given in Table 6. Figure 23 shows the power curve for stall and pitch control.

Table 6. Relative comparison of the stall and the pitch control

Stall control	Pitch control
<ul style="list-style-type: none"> - Angle of incidence of wind is increased causing decrease in lift-to-drag ratio. - Blades designed in a way that at high wind speeds, the rotational speed or the aerodynamic torque reduces, and thus the power production decreases with increasing wind speed above a certain value. - Limited capital cost of the turbine - Lower maintenance - Increasing power up until the rated wind speed, beyond which it sees lower power than rated power until the cut-out speed - Higher vibration and noise. 	<ul style="list-style-type: none"> - Decrement in angle of incidence of wind causes decrease in lift-to-drag ratio. - Equipped with an active control system that can vary the pitch angle (turn the blade around its own axis) of the turbine blades to decrease the torque produced by the blades in a fixed-speed turbine and to decrease the rotational speed in variable-speed turbines. - Higher maintenance and capital cost - Usually employed for high wind speeds only (usually above the rated speed) - Increasing power up until the rated wind speed beyond which it sees constant power until the cut-out speed - Lower vibration and noise
	

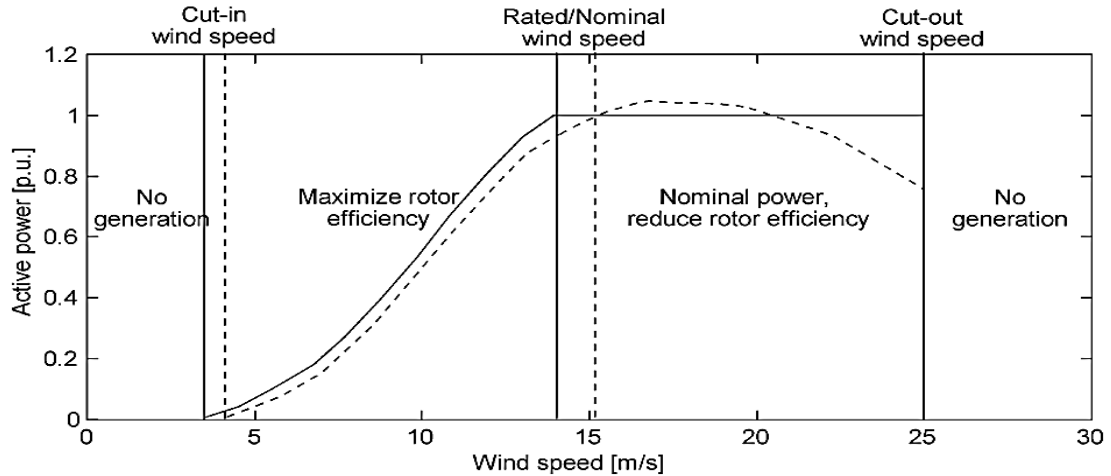


Figure 23. Typical power curves for a fixed speed, stall controlled (dashed) and variable speed, pitch controlled (solid) wind turbines [34]

To accommodate the advantages from the stall and the pitch control mechanism, there is a solution called active stall control where along with the aerodynamic design; blades are furnished with motor to pitch themselves.

Another principle of speed and torque control is furling. It involves aligning the blade rotation plane at some angle to the direction of wind. This can be done along vertical axis as in Figure 10 or horizontal axis as in Figure 24.

E. Generator Types Used in WECS

Traditionally, the SCIGs, the synchronous generators and the dc generators have been used for small scale power generation. The DFIG is currently the most dominant technology for medium and large wind turbines, while the PMSG, the switched reluctance (SR) and the high temperature superconducting (HTS) generators all are extensively researched and developed over the years.

Figure 25 gives a classification of the generators used in the WECS, and their relative comparison is given in Table 7.

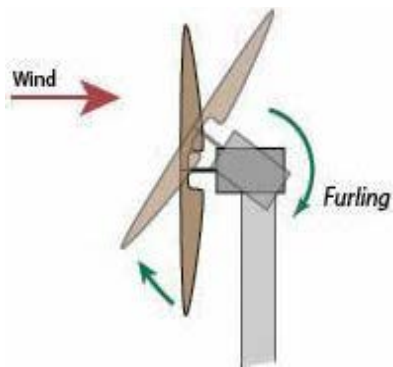


Figure 24. Vertical furling control [46]

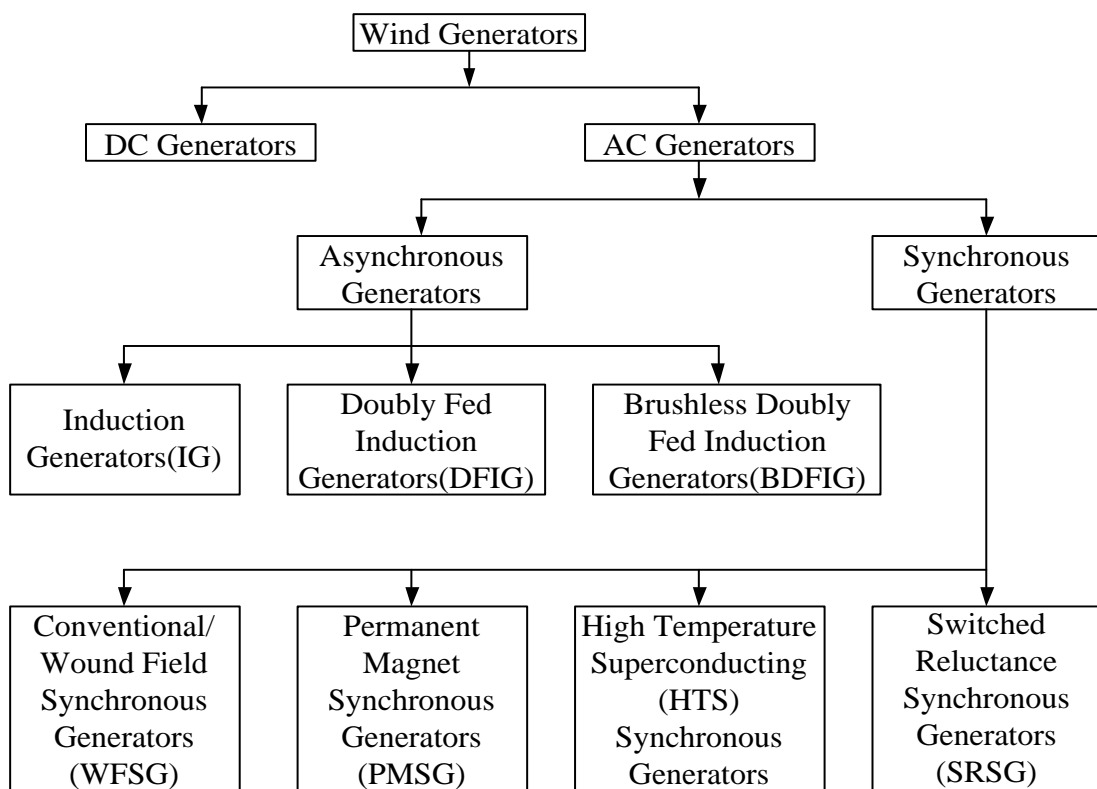


Figure 25. Generators used in the WECS

Table 7. Relative comparison of the wind generators used in WECS [51]

Performance indicator	DC generator	Induction generators		Synchronous generators			
		FSIG	DFIG	Electro-magnet	PMSG	Reluctance	HTS
Speed	Variable	Fixed	Variable	Variable	Variable	Variable	Variable
Power supply	Directly to grid	Directly to grid	Via stator and converter	Totally via converter	Totally via converter	Totally via converter	Totally via converter
Voltage fluctuation	High	High	Low	Low	Low	Medium	Very low
Converter scale	100%	0%	App. 30%	100%	100%	100%	100%
Controllability	Poor	Poor	Good	Good	Good	Good	Very Good
Real and reactive power control	No	Dependent	Separate	Separate	Separate	Separate	Separate
Grid support capability	Low	Low	High	Medium	Very high	Medium	High
Efficiency	Low	Low	High	High	Very high	Medium	Extremely high
Reliability	Poor	Medium	High	High	High	Very high	High
Fault response	Slow	Slow	High	High	High	High	Very high
Cost	Low	Low	Medium	Medium	High	Medium	Very high
Mass saving	Low	Low	High	Medium	Very high	Low	Extremely high
Suitability	Low power, residential turbine	Small wind application	Medium-large wind turbines	Small-medium wind turbines	Direct drive small-medium wind turbine	Early stage	Large wind turbine early stage

F. Power Electronics in WECS

The VSWT technology is actually based on the power electronics. With the advancement in semiconductor fabrication technology along with their modular design, has facilitated the use of power electronic devices in high voltage and high power level with high switching frequency. Table 8 shows the comparison of ratings among the basic power electronic units like GTO, IGCT, BJT, MOSFET and IGBT. The Rectifiers, inverters and frequency converters are made of these units. These days IGBT is the most popular choice for its high frequency operation that enables better control. IGBT is used to form self-commutated power converters. They can work on controlling the current or voltage. These converters are named according to the parameter they are controlling. Figure 26 shows current source converter (CSC) and voltage source converter (VSC).

Table 8. Rating comparison of the power electronic components [52]

	Switch types				
	GTO	IGCT	BJT	MOSFET	IGBT
Voltage ¹ (V)	6000	6000	1700	1000	6000
Current ² (A)	4000	2000	1000	28	1200
Switching frequency ^b (kHz)	0.2-1	1-3	0.5-5	5-100	2-20
Drive requirement	High	Low	Medium	Low	Low

1. Maximum output rating
2. Operational range

As per the converter requirement, the VSWTs are divided into two types, namely, a) full scale converter and b) partial scale converter. They are described in brief below,

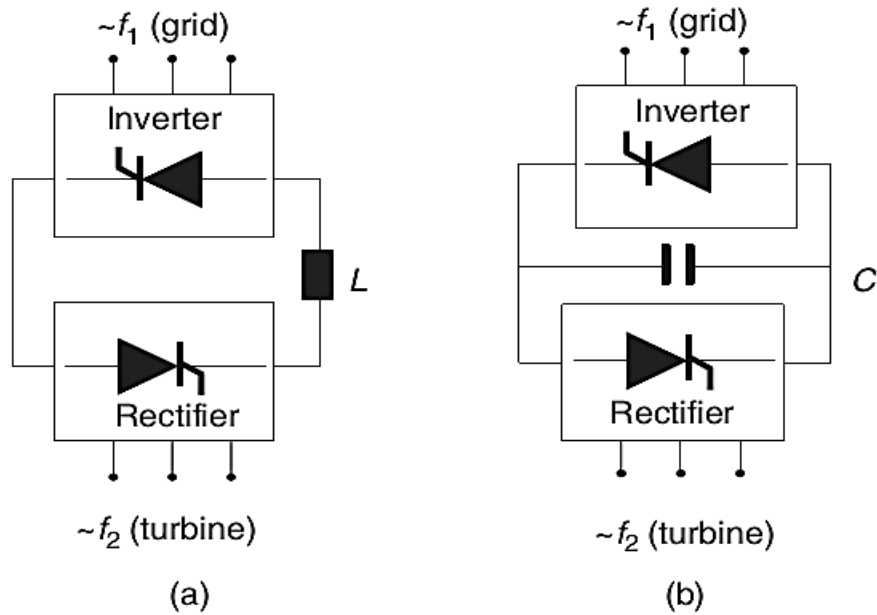


Figure 26. Types of self-commutated power converters for wind turbines: (a) a current source converter and (b) a voltage source converter [52]

Full scale converter: In this type of arrangement, the total generated power is conditioned and it is passed through converters. This gives a full speed range of operation and complete control over real and reactive power. Gear box can be avoided by using direct drive system with the full scale converter. This will enhance efficiency and reduce the cost. The drawbacks are the higher cost of converter and their associated losses. If there is any problem with the converter then the power delivery is fully hampered. WFSG, PMSG, switched reluctance (SR) generator and sometimes SCIG need full scale converter for their operation. Figure 27 shows a diagram for a full scale converter topology for WECS.

Partial scale converter: The Induction generator comes with the advantage of slip power recovery. Which means the rotor can be connected to external circuit to extract

power from it. As the power is fed from the rotor as well as stator, this kind of generator is called doubly fed induction generator (DFIG). The stator is directly connected to the grid but the power through the rotor is conditioned through converters to gain control over voltage, frequency and output power. Most of the power is transferred to the grid via stator and only $\pm 30\%$ of the nominal power is handled by rotor circuit. So only a partially rated converter is enough for its operation. This essentially slashes down the power converter cost and loss associated with converter switching. Brushless DFIG (BDFIG) and cascaded DFIG, the two variant of DFIG, also use partially rated converter. Figure 28 shows a partially rated converter topology.

Frequency converters: The VSWT generators produce a frequency which doesn't match with the grid frequency. To connect the wind turbines to the grid, frequency matching is required. This job is executed by frequency converters. There are a few types of converters available. They are listed below,

- Back-to-back converters;
- Multilevel converters;
- Tandem converters;
- Matrix converters;
- Resonant converters

Some frequency converters are shown in Figure 29.

Back to back converter is very popular. But other converters like multilevel and matrix converters are gaining popularity. Extensive research is going on with designing low cost high efficiency converter topology.

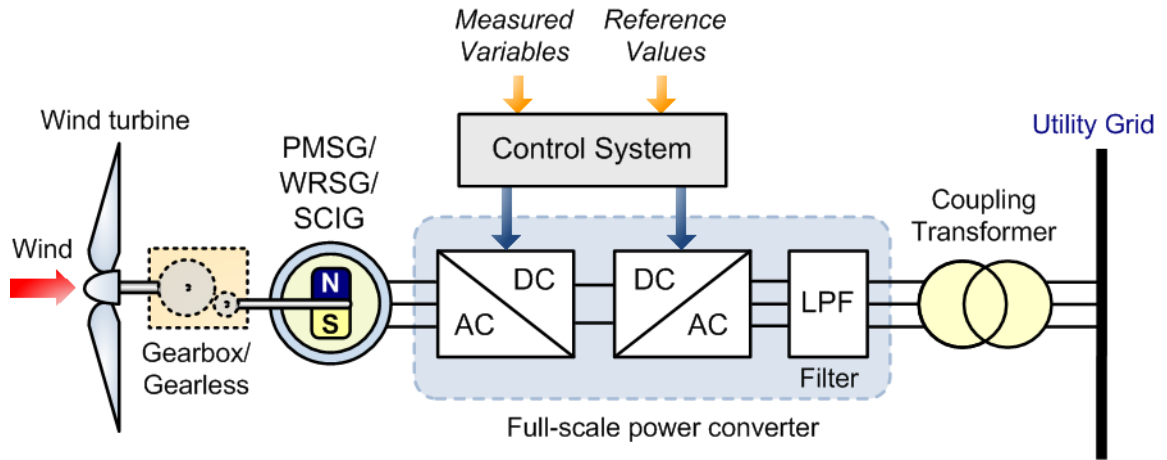


Figure 27. Full scale converter WECS [53]

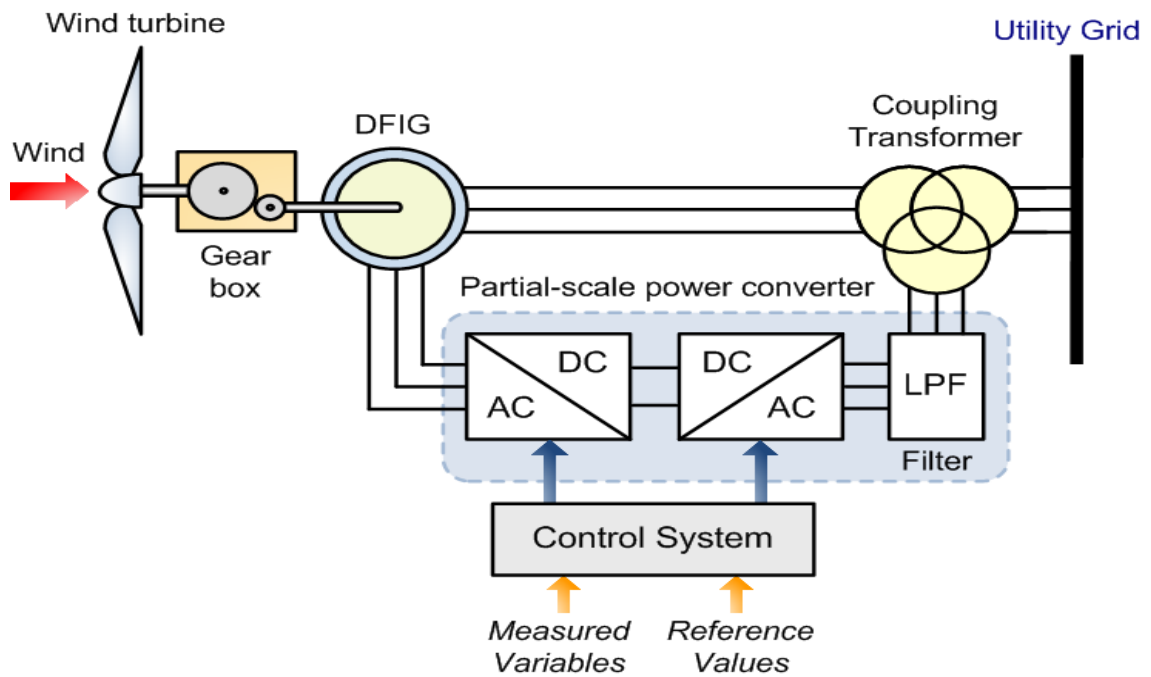
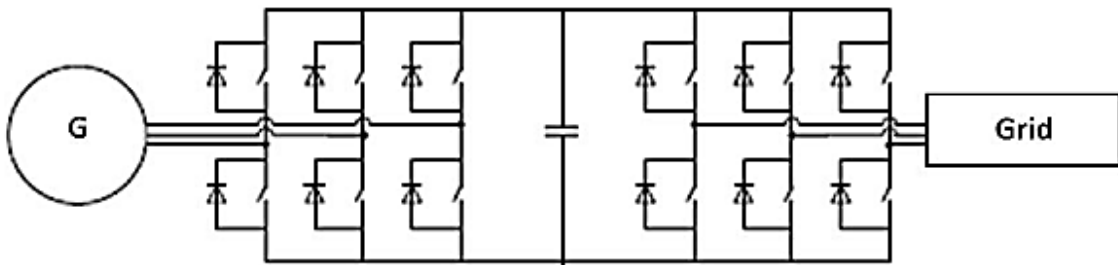
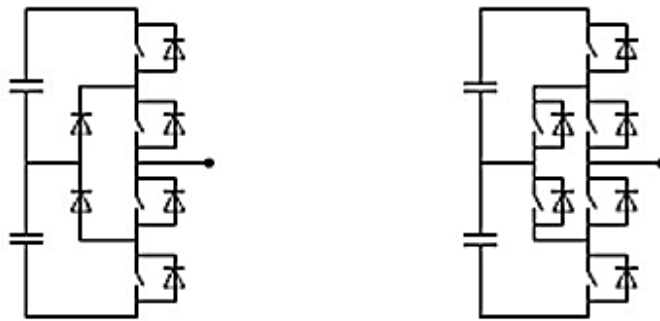


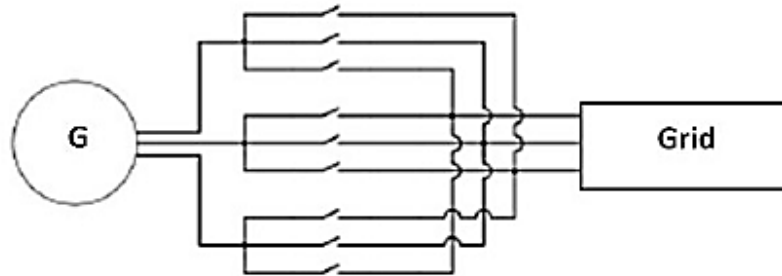
Figure 28. Partially rated converter WECS [53]



(a) Back-to-Back PWM converters



(b) Multi-level converters



(c) Matrix converters

Figure 29. Frequency converters [51]

CHAPTER III

FIXED SPEED WIND TURBINE (FSWT) MODELING

To match with the grid frequency, the SCIG based WECS are made to rotate at a constant speed irrespective of the wind speed variation by some mechanical arrangement like pitch control and yaw drive system. The SCIG's rugged and simple construction, mechanical robustness, reliable operation with low maintenance cost and longer lifetime are the reasons for their popularity.

A. Wind Turbine Modeling

The modeling of wind turbine depends on various physical and geometrical aspects. For detailed modeling of wind turbine mechanical system 6 mass drive train [54] representation [54] is used along with equivalent three and two mass drive train system [49]. In this work, the main objective is to analyze system transient behavior at the event of fault. Therefore to keep things simple and focused to objective, a single mass system is considered.

To model rotor aerodynamics, the popular aerodynamic power coefficient or the C_p versus λ method is considered. There are a few models to characterize C_p - λ relation. In this work, the wind turbine MOD-2 model [11], [55] is considered, which is represented by equation (1) and (2)

$$\lambda = \frac{\omega_r R}{V_w} \quad (1)$$

$$C_p(\lambda, \beta) = \frac{1}{2} (\lambda - 0.022\beta - 5.6) e^{-0.17\lambda} \quad (2)$$

where λ - tip speed ratio

ω_r - the angular mechanical speed

R - blade radius

V_w - wind velocity

C_p - power coefficient or Betz coefficient

β - blade pitch angle.

The relationship between C_p and λ is shown in Figure 30 for different values of β .

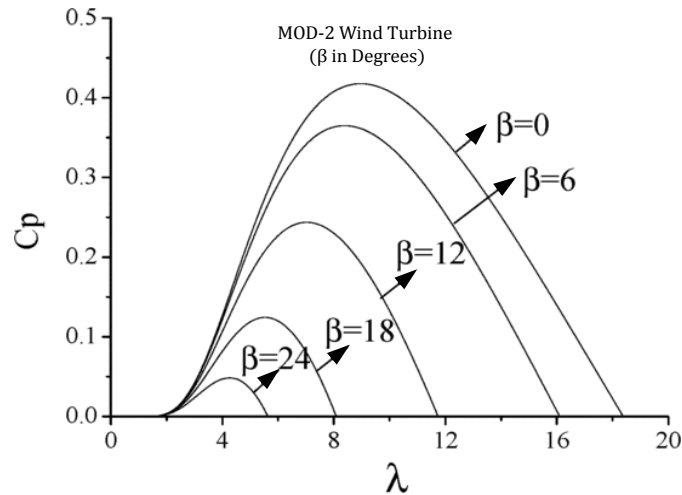


Figure 30. C_p - λ curves for different blade pitch angles (used in FSWT)

The commonly used mathematical relation for the mechanical power harnessed from the wind can be expressed as follows [56],

$$P_w = \frac{1}{2} \pi \rho R^2 V_w^3 C_p(\lambda, \beta) \quad (3)$$

where P_w - extracted power from the wind,

ρ - air density.

The wind turbine parameters used in this work is given in Table 9 [2].

Table 9. Wind turbine data

Characteristic	Value
Turbine Type	3 blade horizontal axis
Radius	46m
Rotor speed	18 rpm
Air density	1.225 kg/m ³
Cut in wind speed	4 m/s
Rated wind speed	Approximately 12 m/s
Tower height	About 100m

B. Wind Generator Modeling

An induction machine is considered as the wind generator. It is modeled using following equations [12], [55], [57], [58] in arbitrary reference frame:

$$V_{ds} = R_s i_{ds} + \frac{d\phi_{ds}}{dt} - \omega \phi_{qs} \quad (4)$$

$$V_{qs} = R_s i_{qs} + \frac{d\phi_{qs}}{dt} + \omega \phi_{ds} \quad (5)$$

$$V'_{qr} = R'_r i'_{qr} + \frac{d\phi'_{qr}}{dt} + (\omega - \omega_r) \phi'_{dr} \quad (6)$$

$$V'_{dr} = R'_r i'_{dr} + \frac{d\phi'_{dr}}{dt} + (\omega - \omega_r) \phi'_{qr} \quad (7)$$

$$\varphi_{qs} = L_s i_{qs} + L_m i'_{qr} \quad (8)$$

$$\varphi_{ds} = L_s i_{ds} + L_m i'_{dr} \quad (9)$$

$$\varphi'_{qr} = L'_r i'_{qr} + L_m i_{qs} \quad (10)$$

$$\varphi'_{dr} = L'_r i'_{dr} + L_m i_{ds} \quad (11)$$

$$L_s = L_{ls} + L_m \quad (12)$$

$$L'_r = L'_{lr} + L_m \quad (13)$$

$$T_e = \frac{3}{2} p \left(\varphi_{ds} i_{qs} - \varphi_{qs} i_{ds} \right) \quad (14)$$

Subscript d and q refers to direct and quadrature axis and subscript s and r refers to stator and rotor quantity. Here φ is the flux linkage, R is the resistance and ω is the angular frequency. Equivalent diagrams for d and q axis are shown in Figure 31 and Figure 32 respectively.

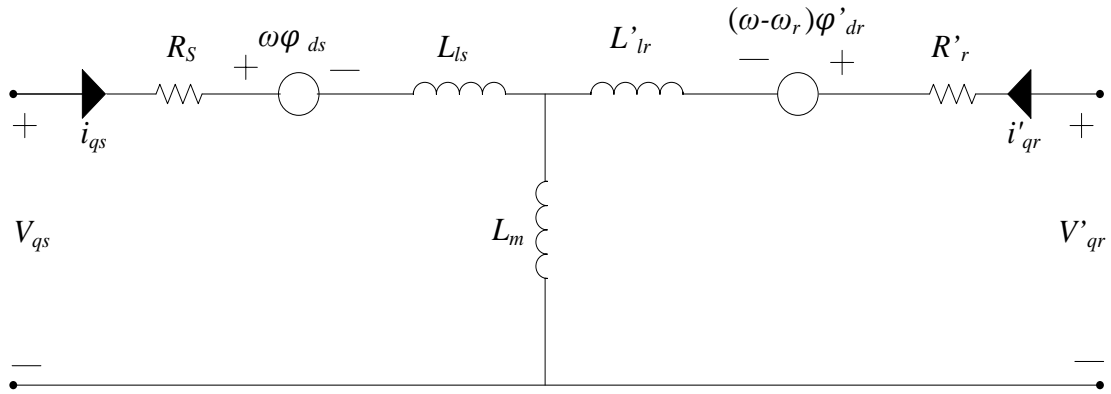


Figure 31. Arbitrary reference frame equivalent d-axis model of 3 phase symmetrical induction machine based wind generator

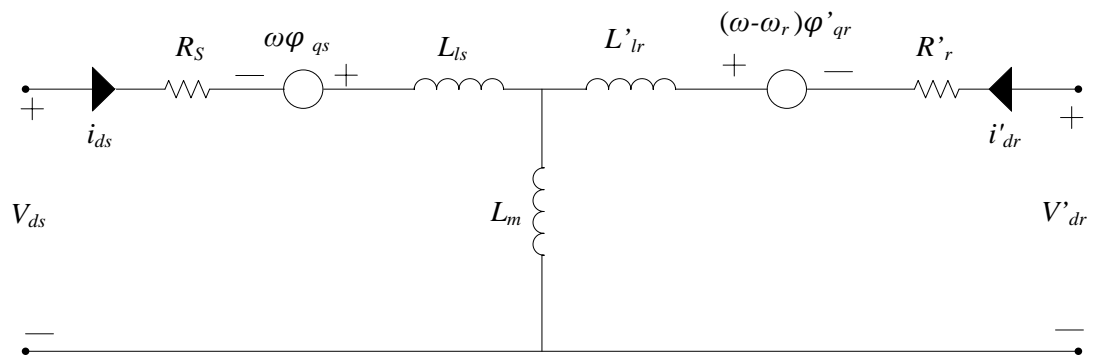


Figure 32. Arbitrary reference frame equivalent q-axis model of 3 phase symmetrical induction machine based wind generator

CHAPTER IV

TEST SYSTEM MODEL

To illustrate the effectiveness of the proposed BFCL and to make a performance comparison between the BFCL and the SDBR, a test system is considered, which is described below.

A. Description of Test System under Analysis

Figure 33 shows the one line diagram of the test system model. This double circuit grid connected transmission line system is used in literature [3], [24], [25]. A 2 MW induction machine is used as a wind generator. A fixed capacitor of 0.005 pu reactive power capacity, is connected to the generator terminal to provide reactive power to the generator and to ensure unity power factor during normal operation. The wind generator is connected to PCC through a step up transformer. The PCC is connected to grid via a double circuit transmission line and then a short transmission line. Each of the line of the double circuit line is identical. Circuit breaker is connected at each side of the double circuit lines for fault protection. Line and other parameters are shown in the figure. The most vulnerable point of system is found to be the point on the double circuit line close to the PCC marked by F1 in Figure 33.

The wind generator parameter used in this work is listed in Table 10 [61]. Machine parameters are calculated in machine base. The test system equivalent diagram considering fault scenario and equivalent circuit of an induction generator are depicted in Figure 34.

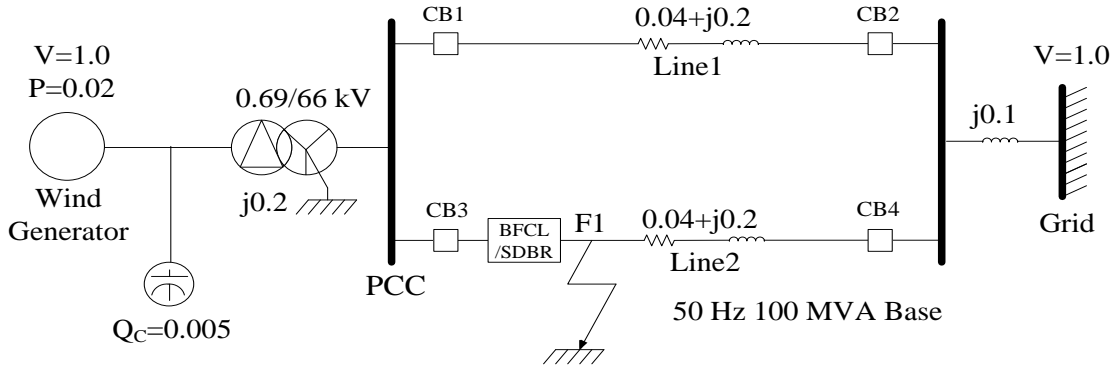


Figure 33. Detailed test system model

Table 10. Wind generator parameters

Generator characteristic	Value
Nominal Power (P)	2 MW
Rated Voltage (V)	690 V
Stator Resistance (R_s)	0.00488 pu
Stator Reactance (X_s)	0.09241 pu
Rotor Resistance (R_r)	0.00549 pu
Rotor Reactance (X_r)	0.09955 pu
Mutual Reactance (X_m)	3.95273 pu
Inertia Constant (H)	0.5 s

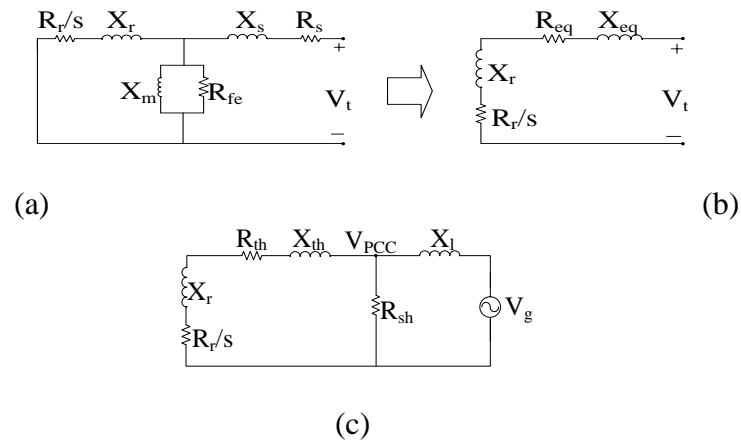


Figure 34. (a) Induction machine based wind generator equivalent and (b) simplified circuit. (c) Equivalent system diagram after fault

CHAPTER V

BRIDGE TYPE FAULT CURRENT LIMITER (BFCL)

The details of the configuration, operation, design consideration and control strategy of the proposed BFCL are as follows.

A. BFCL Configuration

A modified configuration of BFCL, different from the one used in [24], [25], is used in this work. The BFCL is composed of two sections, namely the bridge part and the shunt path.

The first part is essentially the bridge part composed of four diodes $D_1 \sim D_4$ (Semikron SKNa 402 [62]) in bridge configuration, a small value dc reactor L_{dc} equipped with a parallel free wheeling diode D_5 (Semikron SKNa 402) in series with an IGBT switch (CM200HG-130H [63]) as shown in Figure 35. The IGBT switches normally come in a

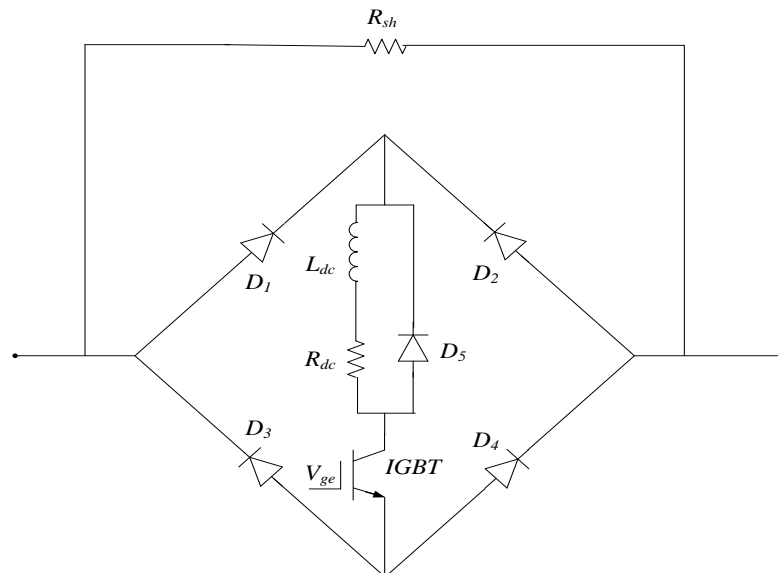


Figure 35. Per phase configuration of modified BFCL.

package with free wheeling diode which is not shown here. Also, to include the inherited resistance of inductor, a very small value resistor R_{dc} is considered. The second part is a shunt branch composed of a resistor R_{sh} designed to meet the circuit criteria. A resistor and an inductor in series were used in the shunt path [24], [25]. But here only the resistor is used. This is because when the shunt path is withdrawn after breaker opening; the reactor discharges the stored energy and results in rise of current. This deteriorates the fault recovery performance. The BFCL is connected in series with transmission line, and placed in between the circuit breaker and transmission line. Figure 36 shows Matlab implementation of per phase BFCL.

B. BFCL Operation

During normal operating condition of the system, the IGBT remains closed as its gate signal V_{ge} is at high state. For one half cycle of electrical frequency, the $D_1-L_{dc}-R_{dc}-D_4$ path carries line current and for the other half cycle, current is carried by $D_2-L_{dc}-R_{dc}-D_3$.

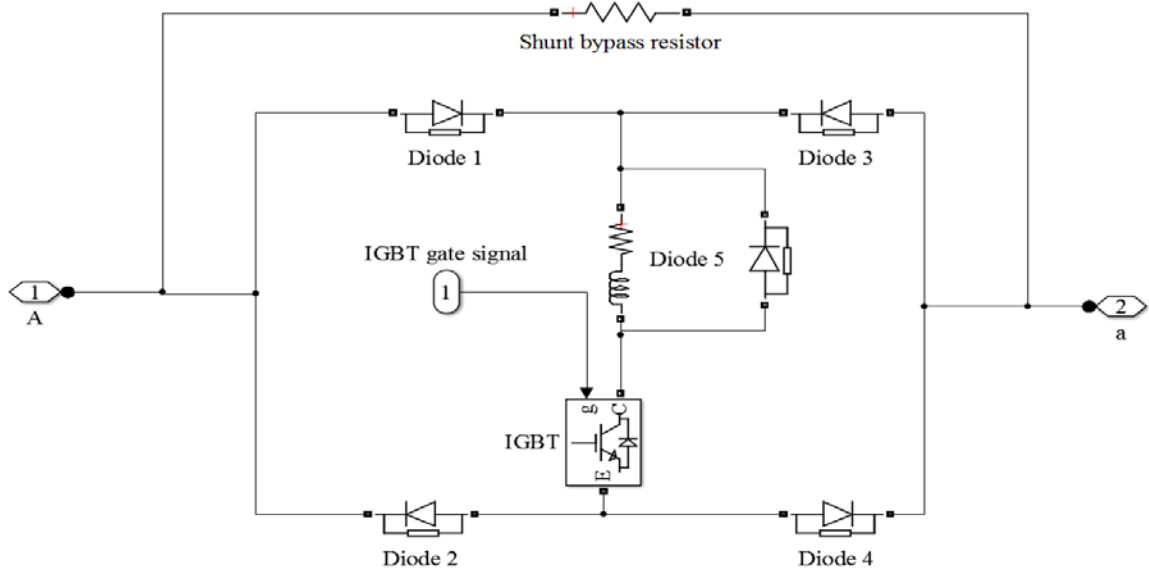


Figure 36. Matlab implementation of per phase modified BFCL

So, the current through the dc reactor L_{dc} flows in the same direction for both of the half cycles and the current through this inductor is dc. We know that inductors offer no impedance to dc, so for this dc current the inductor path acts as a short circuit. The dc reactor is charged to the peak current and voltage drop due to current ripple is very small compared to line voltage level. The dc reactor inherited resistance and IGBT turn-on resistance incurs some voltage drop, as they are connected in series to line. But this voltage drop is quite negligible compared to line drop and has ignorable significance. For these reasons, the bridge has no impact on steady state operation. The impedance of the shunt path is high enough, so except very small leakage current, during normal operation line current flows through the bridge fully.

At the event of fault, line current tends to increase but the reactor limits its increasing rate at the first instant and the IGBT switch is saved from sharp di/dt rate at the starting of fault. As the line current through the dc path i_{dc} , crosses the predefined maximum permissible current i_{th} , the BFCL control system forces the IGBT gate voltage V_{ge} to low state and the IGBT is turned off. The bridge is withdrawn from the system and the bypass or shunt path takes the flow of current. The shunt path limits the fault current and consumes excess energy from the wind generator and fault ride-through is achieved.

When the IGBT switch is turned off, the free-wheeling diode of the dc reactor and the snubber of the IGBT switch provide free path to discharge accumulated energy in them.

After the circuit breaker opening, the system starts to recover and the voltage rises at the buses. As the voltage at the PCC reaches to some predefined reference value, V_{ge} goes to the high state turning on the IGBT switch, and the system is brought back to the normal operating state. The controller used for the BFCL is shown in Figure 37. It is

composed of two comparators and a signal accumulator. Signals from two comparators are collected, and an appropriate gate control signal V_{ge} is sent via signal accumulator.

Matlab implementation of per phase BFCL controller is shown in Figure 38.

C. BFCL Design Considerations

During normal operation, each line of the double circuit line carries equal amount of power. To continue the normal operation or to ensure the least disturbance at fault, the BFCL should consume power equal to the amount which the faulted line carries in prefault situation. The power consumed by the BFCL at postfault is given by equation (15) and (16)

$$P_{BFCL} = \frac{V^2 P_{CC}}{R_{sh}} \quad (15)$$

$$P_{BFCL} \approx \frac{P_G}{2} \quad (16)$$

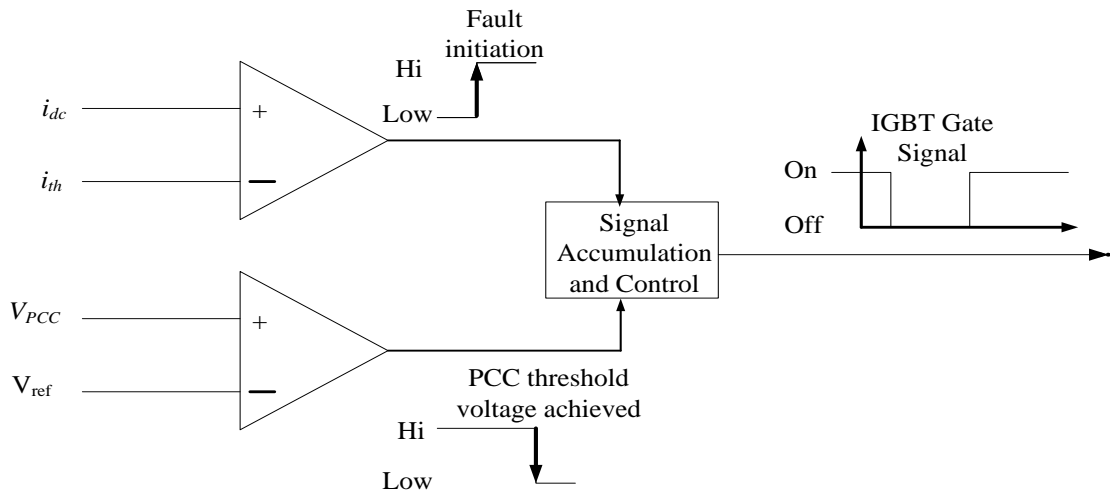


Figure 37. BFCL controller

where P_{BFCL} and P_G are power consumed by the BFCL and power delivered by the generator, respectively, V_{PCC} and R_{sh} are the PCC voltage and the shunt path resistance, respectively. The value of the shunt resistance is approximated from equation (15) and (16) and the optimum value was found to be approximately 1.1 pu.

D. BFCL Control Strategy

There are handful parameters that can be used in the BFCL controller. The line current, line voltage, wind generator terminal current, active and reactive powers through line are probable candidates. Here, the dc current through the dc reactor is used to control the IGBT switch. The dc reactor is charged to a certain current level at normal operation. At fault this current tends to go high and its rate of rise is faster than the line current or other parameters. So, by using this parameter, faster control is possible. When this dc current crosses the threshold current value due to fault occurrence, the IGBT switches are turned off and current in the bridge is bypassed to the shunt path.

When the circuit breakers are opened, the system recovers and goes to the steady state. As the PCC voltage tends to cross the predefined threshold value, the IGBT

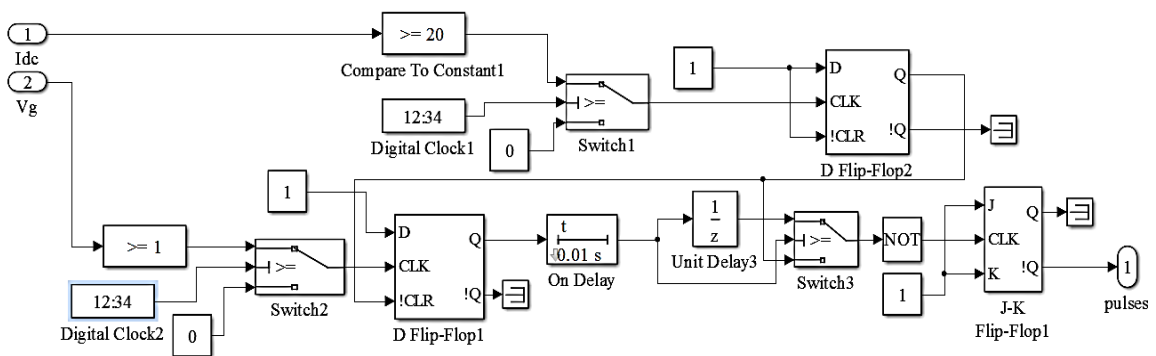


Figure 38. Per phase BFCL controller implementation in MATLAB

switches are closed and again current flows through the dc reactor. In a synchronous generator, fault current through line tends to be very high compared to line current and stays high until fault is isolated by breaker opening. But for an induction machine based wind generator case, the fault current through line tends to fluctuate. That's why two different parameters are used for the BFCL controller as from apparent Figure 37.

CHAPTER VI

SERIES DYNAMIC BRAKING RESISTOR (SDBR)

To show the effectiveness of the proposed BFCL, its performance is compared with the SDBR. The SDBR is a proved technology, and previous studies show that it has the ability to improve the fault ride-through capability and enhance transient stability [19], [31], [64] of the wind generator systems. The SDBR was modeled like [19], and placed in the same position where the BFCL was placed in the test system model. The details of the configuration, operation, design consideration and control strategy of the SDBR are provided below.

A. SDBR Configuration

The SDBR is basically a resistor with a bypass switch in parallel with it as shown in Figure 39. This paper considers this switch to be IGBT based (CM200HG-130H) due to its very fast response and modular design. MATLAB implementation of SDBR is shown in Figure 40. Like the BFCL, this is also connected in series with the transmission line.

B. SDBR Operation

During normal operating condition, the SDBR would operate with V_{ge} at high state, making the IGBT switch closed. The line current will flow through the IGBT switch

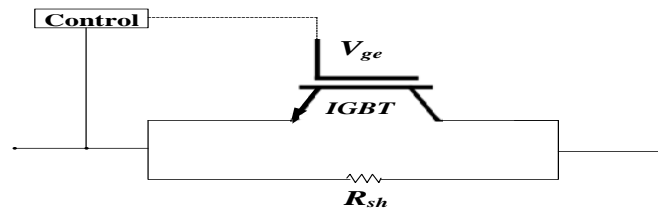


Figure 39. Per phase SDBR topology

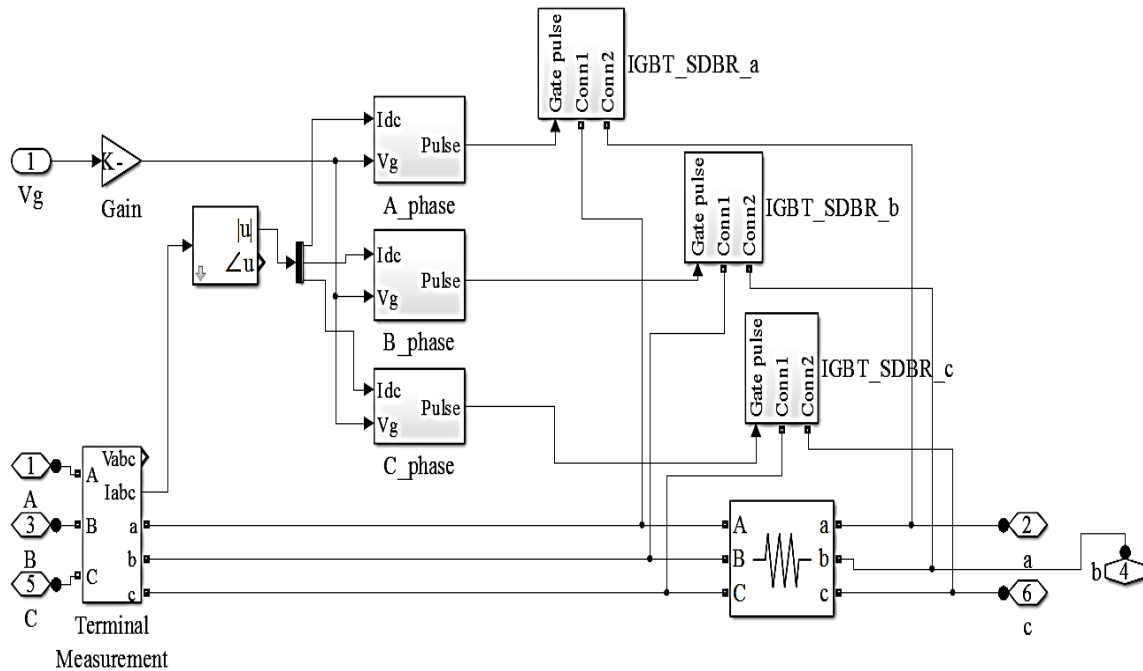


Figure 40. MATLAB implementation of SDBR

bypassing the braking resistors placed in parallel. At the event of fault, V_{ge} goes to low state opening the IGBT switch, and shunt resistor will be dynamically inserted into the network. The line Current would then flow through the inserted resistor for the faulty condition and impeded by the resistor. When the desired voltage level is achieved at PCC after opening of the circuit breakers, V_{ge} will be in low state and the switch would be closed. Then the system would return to steady state and resume its normal operation.

C. SDBR Design Considerations

The SDBR concept works by contributing directly to the balance of active power. During a fault, the SDBR system dynamically inserts a resistor in the generation circuit, thus increases the voltage at the terminals of the generator and mitigates the destabilizing electrical torque by consuming active power during the fault period. Like the design of

the BFCL, equations (15) and (16) are also used to calculate the value of the braking resistor to make the comparison compatible. The optimum value of resistor, R_{sh} , used in the SDBR was found to be approximately 1 pu.

D. SDBR Control Strategy

The strategy of control used for the SDBR is the same as the one used for the BFCL as shown in Figure 37. Like the BFCL, there is no dc current available in the SDBR. So the line current is taken and its value is converted to corresponding RMS value, i_{dc} . Then this value is compared to the threshold current level i_{th} . Rest of the control procedure is the same as the BFCL. A Matlab implementation of the per phase SDBR controller is shown in Figure 41. This really provides a common platform to compare two similar technologies.

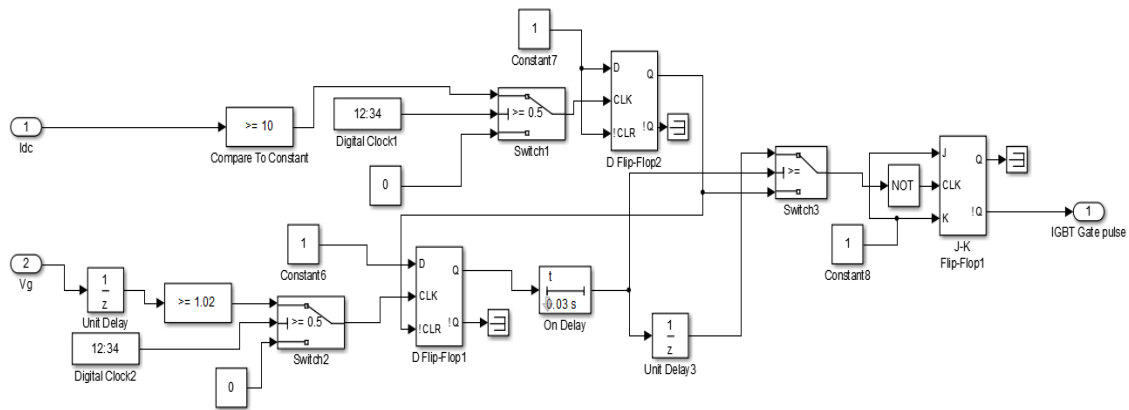


Figure 41. Per phase SDBR controller implementation in MATLAB

CHAPTER VII

SIMULATION RESULTS AND DISCUSSIONS

In this work, simulations were carried out using Matlab/Simulink software. As stated earlier, three kinds of faults are considered in this work. They are 3LG, LL and 1LG faults. Instead of double-line-to-ground (LLG), the LL fault is considered because it is different from the ground fault. All of the faults are temporary type. Simulation results together with detailed result discussions are given below.

A. Assumptions and Considerations

For fault analysis purpose, a fixed wind speed of 12 m/s is considered as it produces rated power. The wind speed is assumed constant for the duration of interest. This is a fair assumption as the fault initiation and recovery happens in a brief period of time, and wind speed doesn't change too much practically within this short time frame. Also this work concentrates on the fault ride through performance rather than the fluctuating wind speed problem. The line parameters are shown in Figure 33. Temporary 3LG, LL and 1LG faults are applied to the system at the point F1 near the PCC at 0.1 s. The circuit breakers on the faulted line open at 0.2 s recloses at 1.2 s. Reclosing of circuit breakers is successful and it refers to a temporary fault type. The simulation time step used for the study is 0.00001 s. In the following section, system responses are shown in a common time span of 0 to 1.5 s. Three different cases are considered in the simulation, which are as follows:

Case A: with no auxiliary controller

Case B: with BFCL

Case C: with SDBR

B. Fault Current Suppression and FRT for 3LG Fault

Figure 42 shows the fault current from line to ground in faulted line. It is seen that the fault current reaches around 7.5 pu calculated in machine base, and it is suppressed around 3 pu with the help of BFCL. This indicates that the fault current from faulted point of line towards ground is suppressed significantly by using the BFCL. This ability enables the use of lower rating circuit breakers.

The current from machine towards the PCC at fault is reduced to less than 1.2 pu from around 3 pu as shown in Figure 43. The BFCL can also suppress fault current through the PCC. In both cases, the BFCL performs better than the SDBR, and sudden jump in current is also prevented.

Figure 44 shows the active power consumed in the BFCL and SDBR. It is seen that from the fault initiation to breaker opening, the BFCL consumes more active power than

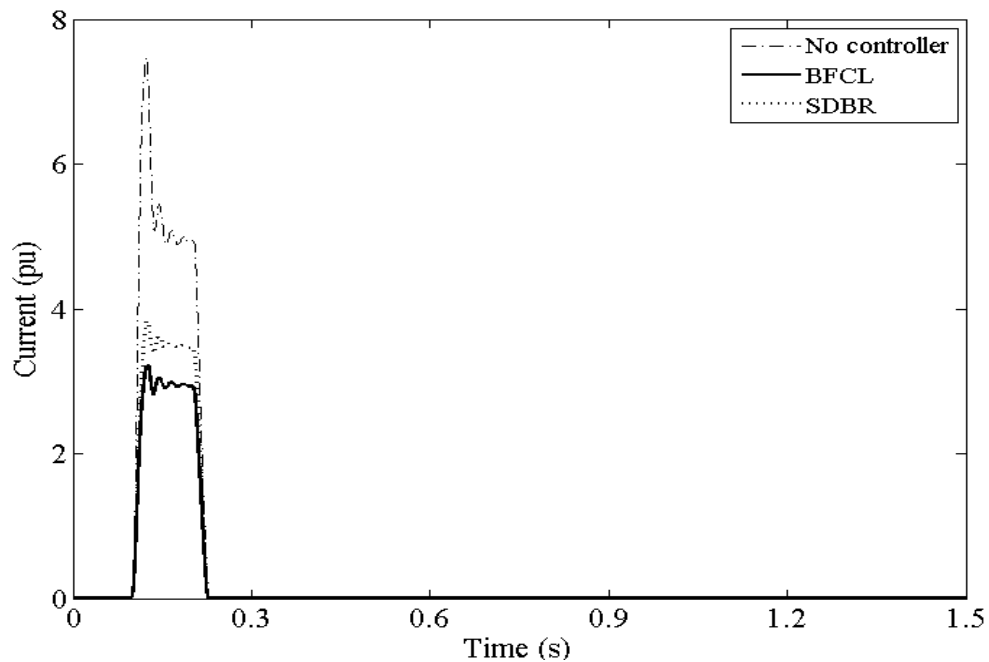


Figure 42. Fault current from line to ground in faulted line for 3LG fault.

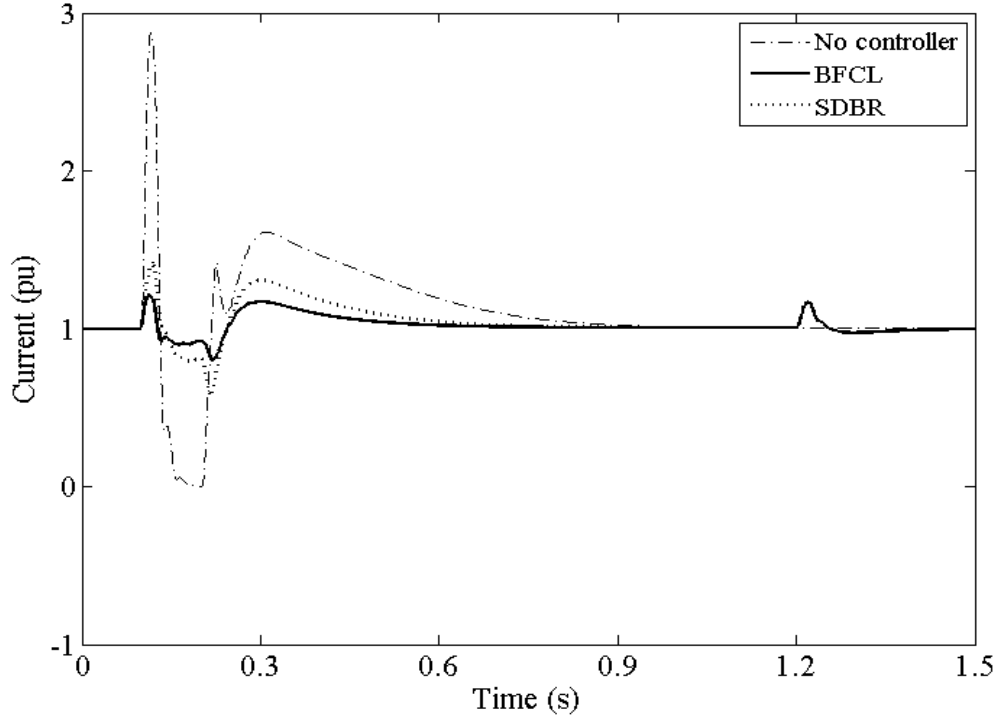


Figure 43. Current at PCC for 3LG fault

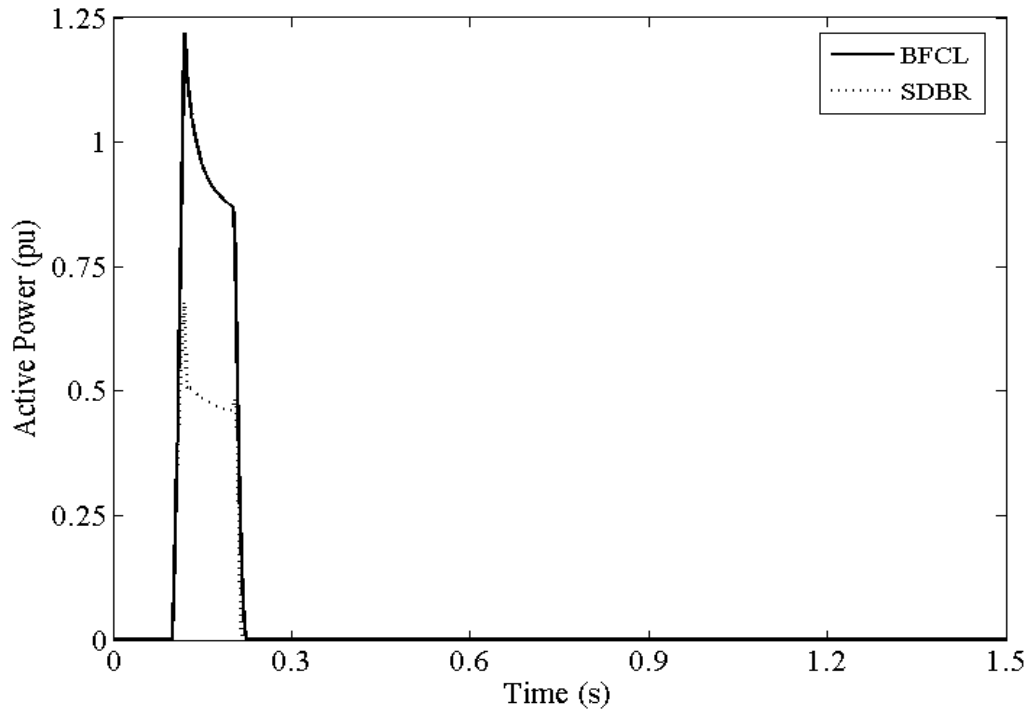


Figure 44. Active power consumed in BFCL and SDBR for 3LG fault

the SDBR which enables the BFCL to perform better. Another thing is to be noted that the BFCL consumes active power only when the IGBT switch in the bridge is open. At normal operating situation, it consumes no active power, thus has no effect in steady state operation.

In Figure 45, the PCC RMS voltage response for the three cases along with the USA grid code is shown. A larger timeframe is considered in this plot to incorporate the grid code. For the uncompensated system or case A, the PCC voltage goes to almost zero and thus violates the grid code. With the BFCL in action (case B), the voltage is maintained over 0.8 pu. The SDBR (case C) can also help maintain the voltage level but the BFCL keeps voltage level at the PCC higher than the SDBR from the fault initiation to breaker opening instant.

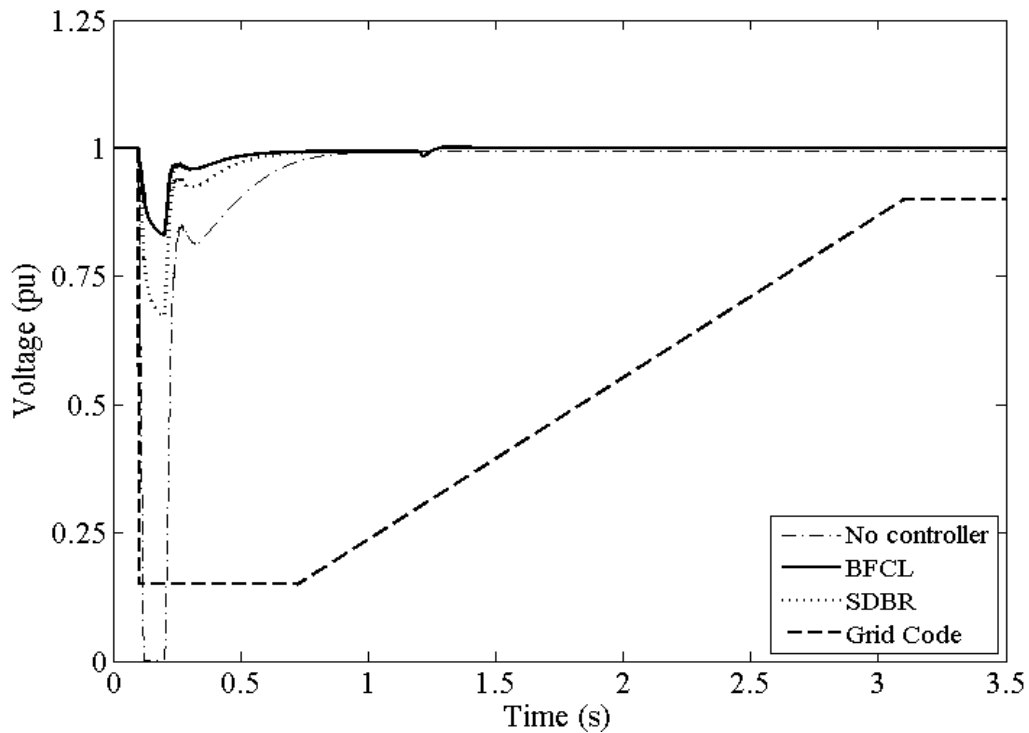


Figure 45. Voltage at PCC for 3LG fault

Figure 46 represents the wind generator terminal voltage response. As there is abrupt rise of current in the event of fault, wind generator terminal voltage faces instantaneous voltage drop. For a clear view, the zoomed fault instant terminal voltage response is shown inside Figure 46. This creates stress on the system especially on the generator. The SDBR can minimize this sudden drop, but the BFCL performs much better than the SDBR in this regard, which is a unique feature of the BFCL. Also, after fault recovery, the BFCL brings terminal voltage level back to the prefault terminal voltage level.

The wind generator speed response is shown in Figure 47. The fault makes wind generator speed go high. This may cause instability if the circuit breaker takes long time to open and proper auxiliary measure is not taken. The BFCL limits the rate of rising of machine speed and ensures better stability. It is more competent to do this than the

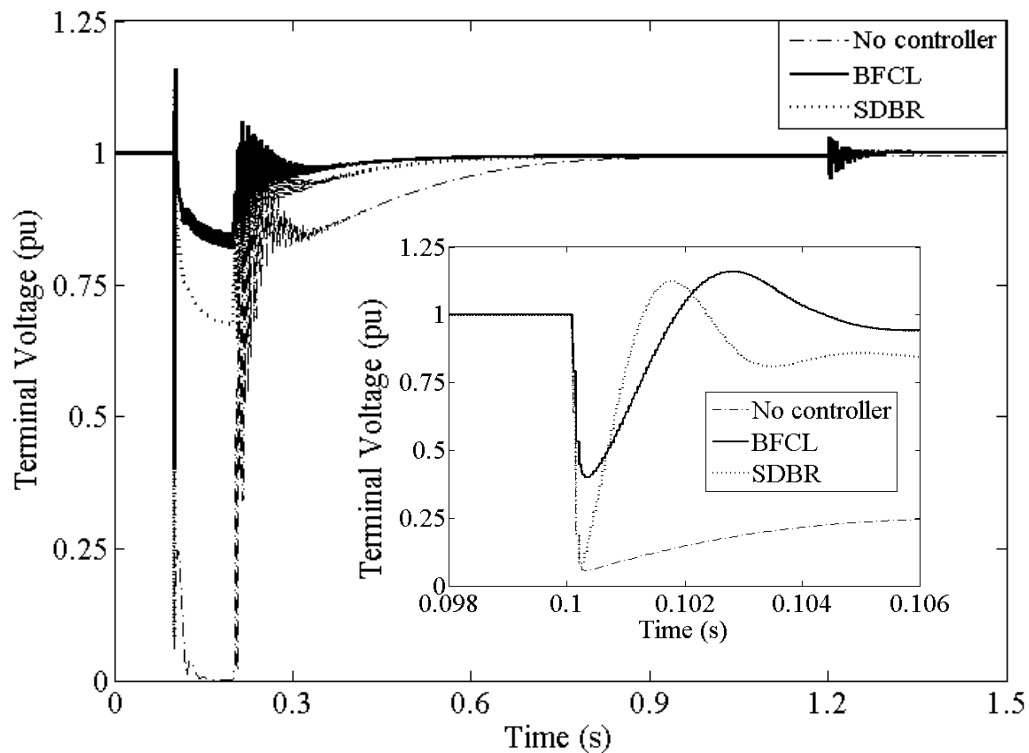


Figure 46. Wind generator terminal voltage for 3LG fault

SDBR. Also, the BFCL brings the machine back to its prefault speed after circuit breaker reclosing.

Figure 48 gives the wind generator electrical torque behavior. There is huge fluctuation in electrical torque caused by fault. With no controller, torque becomes very low. This change of torque is very sharp and harmful for turbine generator system. The BFCL prevents electrical torque to go very low and hinders fluctuation. In this way, it gives better and quicker stabilization. The SDBR performance is not as good as the BFCL in this regard as evident from Figure 48.

Figure 49 and Figure 50 show wind generator active and reactive power response, respectively. During fault the wind generator output active power becomes almost zero. But the BFCL helps to maintain more than half of the rated active power at the PCC

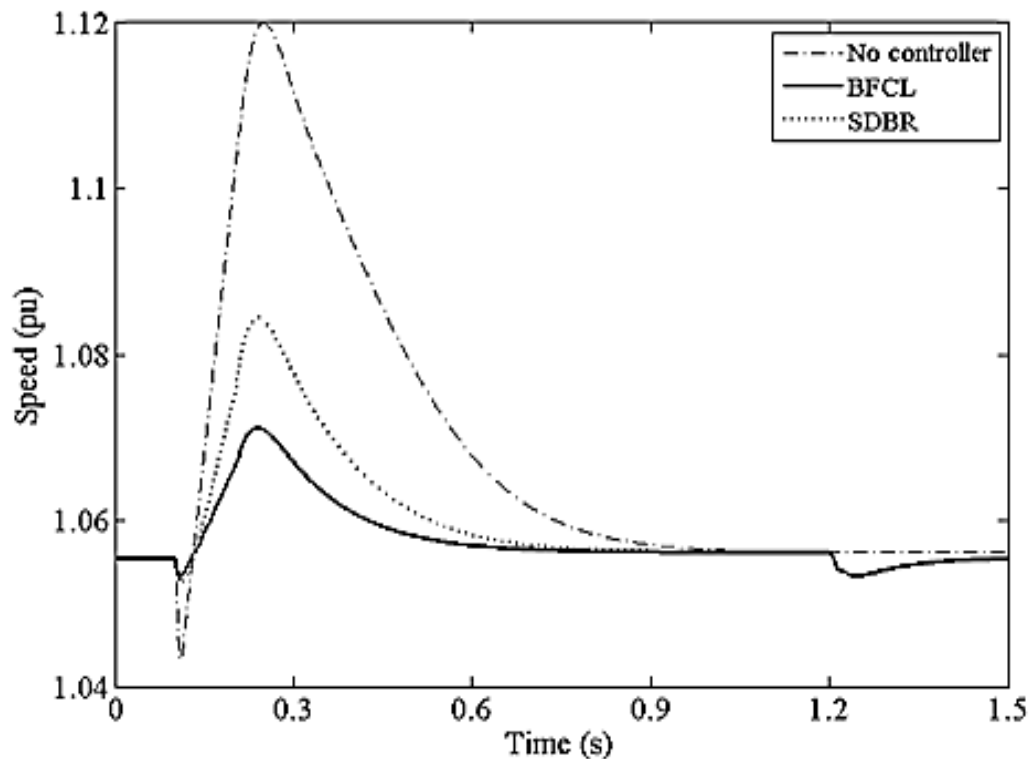


Figure 47. Wind generator speed response for 3LG fault.

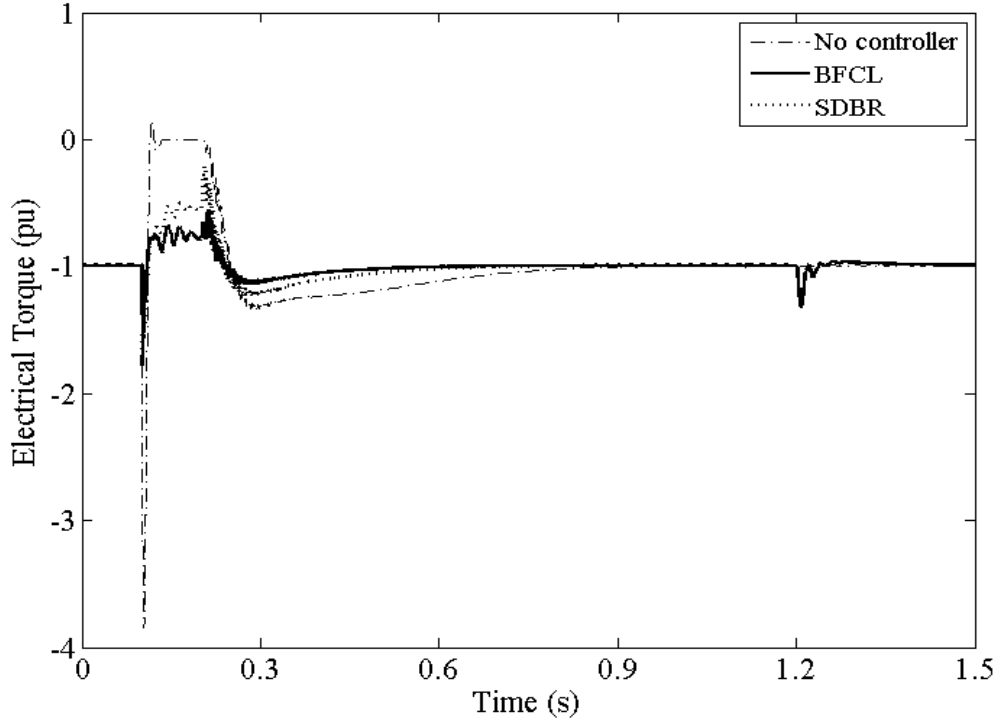


Figure 48. Wind generator electrical torque for 3LG fault.

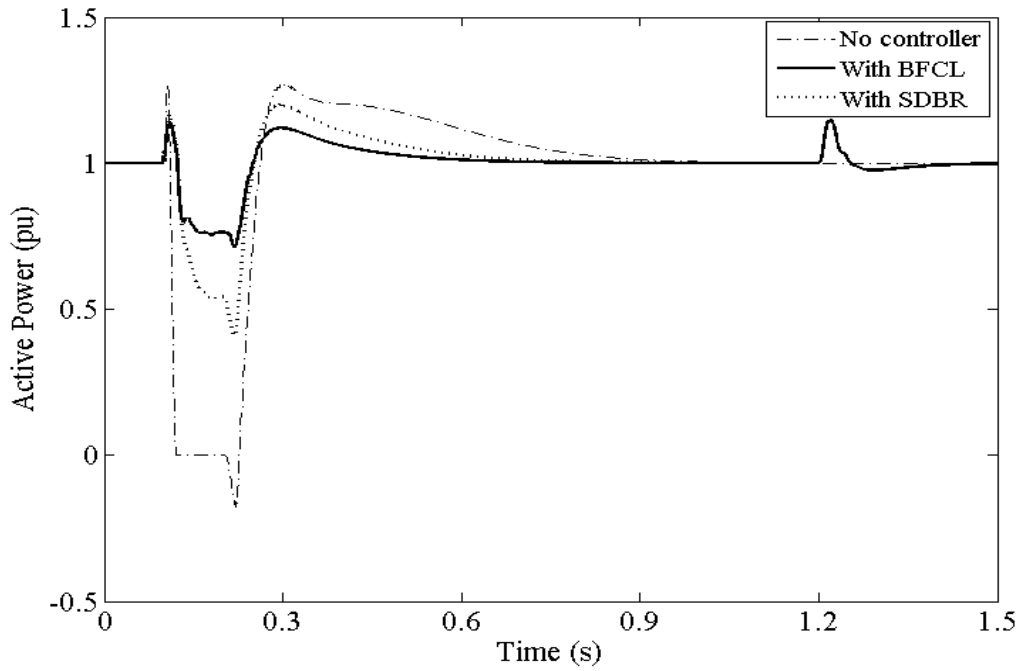


Figure 49. Wind generator active power output at PCC for 3LG fault.

during the fault. The BFCL draws some more active power than the SDBR. From fault instant till breaker opening, the wind generator draws high reactive power. With the BFCL this demand is limited and it is less than that is required with the SDBR. Hence the grid is required to supply lower reactive power and feels lower stress.

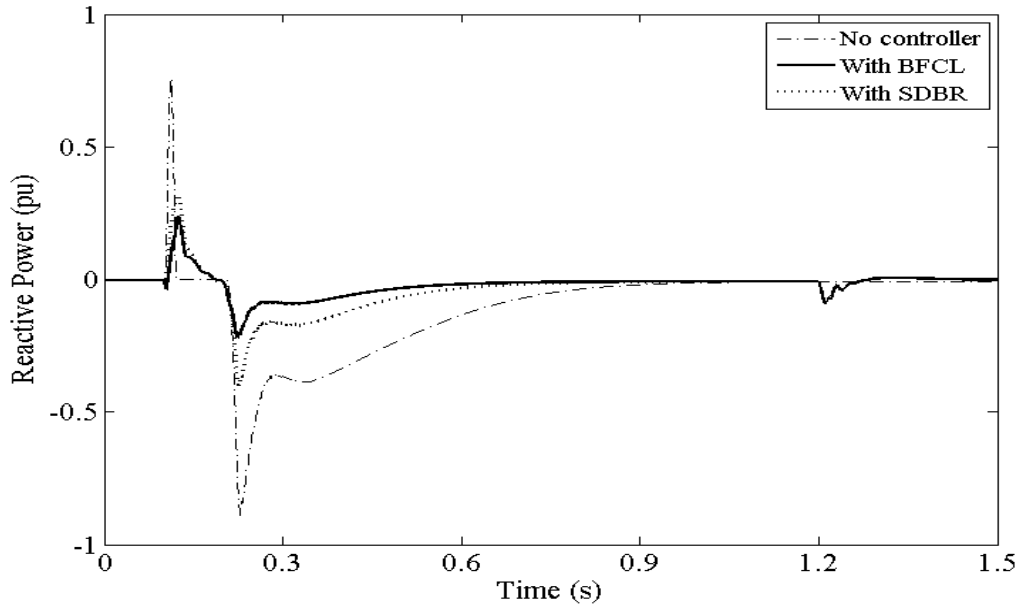


Figure 50. Wind generator reactive power output at PCC for 3LG fault.

C. Fault Current Suppression and FRT for LL Fault

In this subsection, simulation results for LL fault have been shown. The fault is applied between phase a and phase b. The ground connection is not present in this fault. Figure 51 shows the fault current for the LL fault. With no controller this fault current reaches around 4 pu and it is significantly suppressed by BFCL to around 2 pu. SDBR keeps the current level in between the no controller and BFCL case. The curves show that the BFCL performs better than the SDBR.

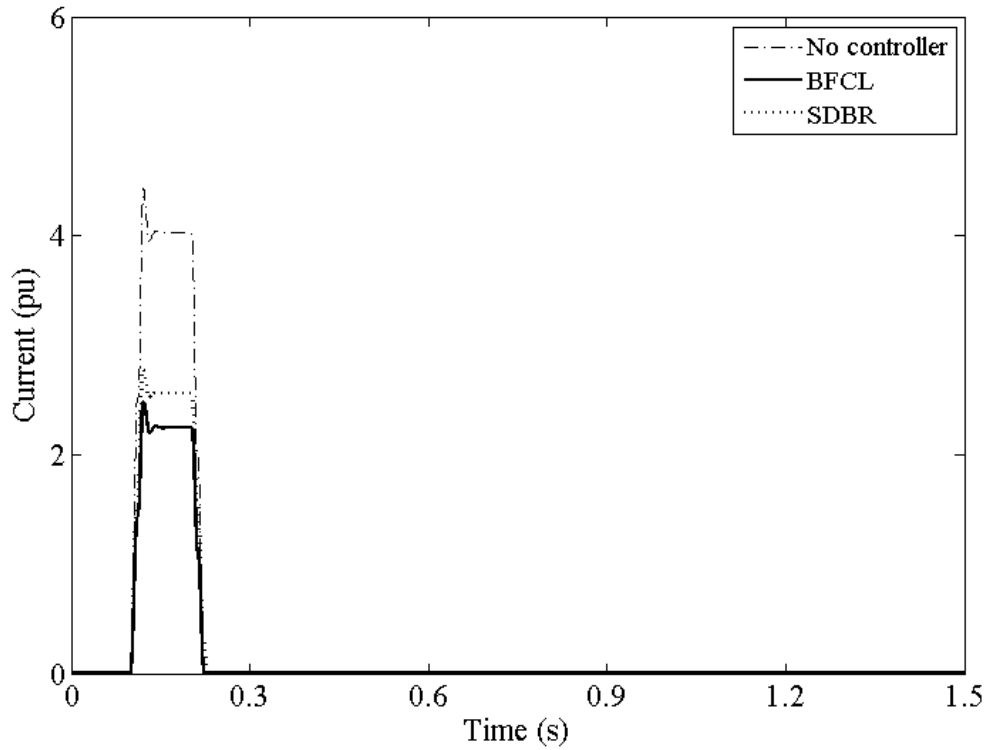


Figure 51. Fault current for LL fault.

The current at PCC at faulted situation and recovery is shown by Figure 52. The fault current at PCC suddenly rises to about 2 pu if no auxiliary measure is used. Also there is a sharp rise of current at the breaker opening. With the SDBR, it rises up to 1.5 pu with longer stabilization time. But for the BFCL, the current at the PCC lies to around ± 0.1 pu.

The PCC rms voltage as shown in Figure 53 comes down to half the nominal value if a LL fault is applied without any controller. Both the BFCL and SDBR help to maintain voltage level higher as compared to no compensator case, but better voltage level offered by the BFCL is noticeable.

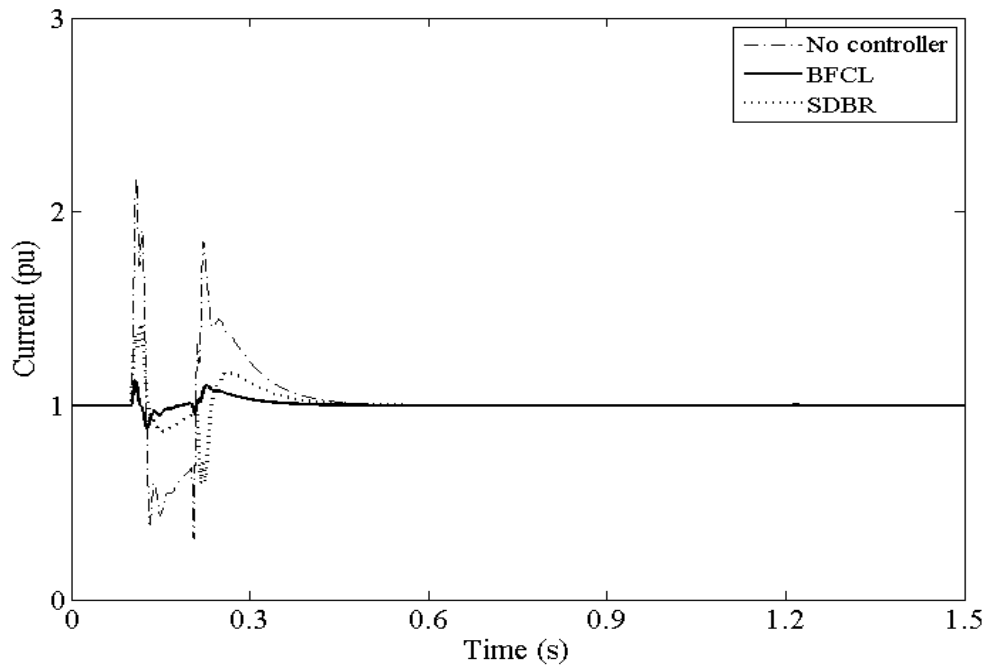


Figure 52. Current at PCC for LL fault

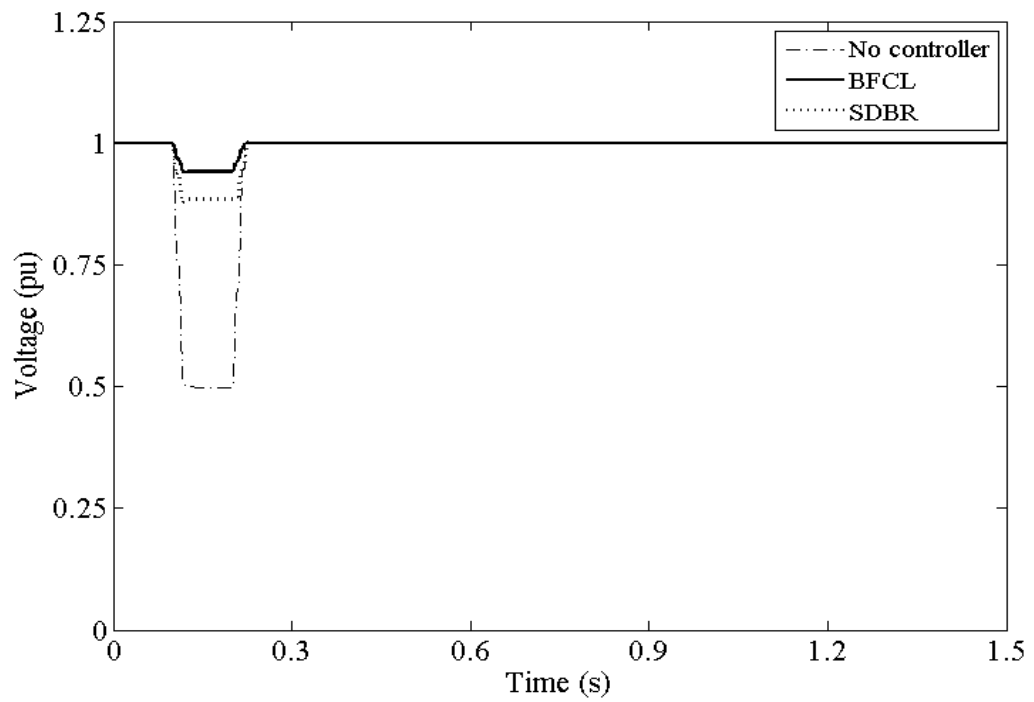


Figure 53. Voltage at PCC for LL fault

Figure 54 represents the per phase voltage waveform at PCC during temporary LL fault situation. It is noticeable from the top waveshapes that during fault the voltages at phase a and phase b become the same in magnitude and phase. The voltage magnitudes in phase a and b go down. The waveshapes in middle of Figure 54 shows that the BFCL keeps both the phase and magnitude of phases a and b almost unchanged. The bottom wave shapes of Figure 54 shows that compared to the BFCL, the SDBR performance is worse.

Figure 55 shows the wind generator terminal voltage response for a LL fault. With no controller the terminal voltage gives very high magnitude fluctuation ranging from 0.05 to 1.05 pu. With the SDBR there is also significant amount of fluctuation from 0.75 to

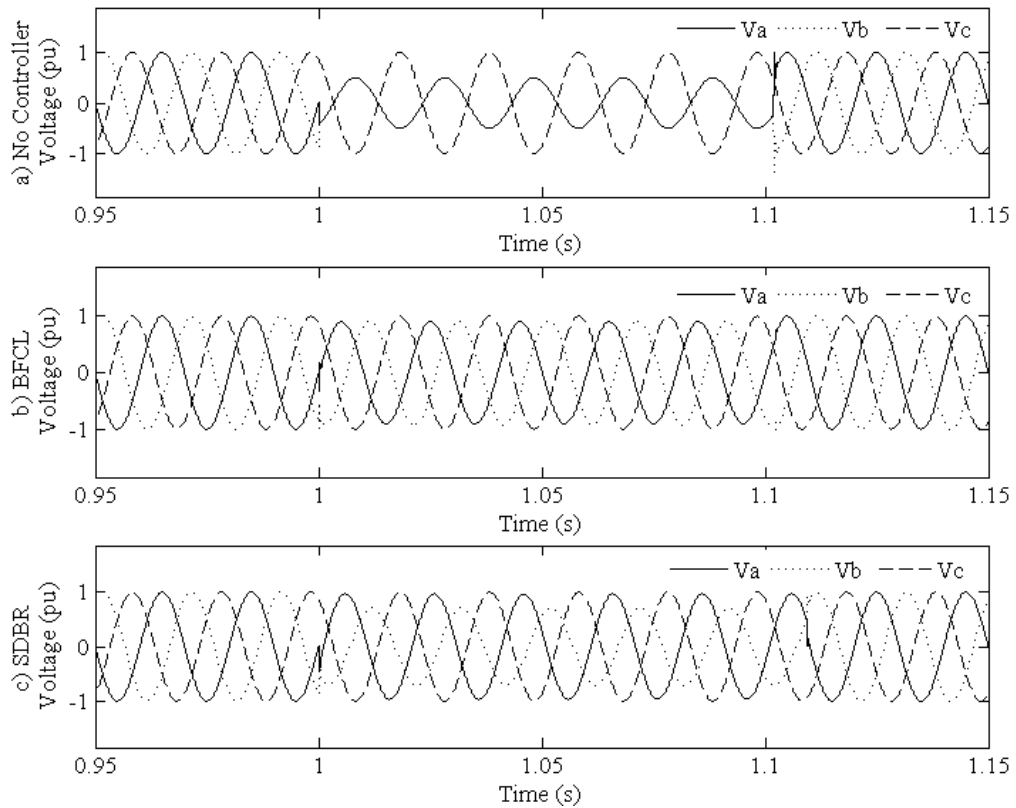


Figure 54. Per phase voltage waveform at PCC for LL fault

1.05pu. But with the BFCL this fluctuation is reduced significantly as evident from the figure.

Figure 56 shows the wind generator speed response after being faced with a line to line fault. The fault in the line makes the generator speed rise fast, and this is a threat to stable operation. With the BFCL in place, the speed cannot go very high as well as the speed fluctuation is kept to the minimum. The SDBR can also minimize rise of speed but the fluctuation is higher than that of BFCL.

The wind generator torque response for LL fault is shown in Figure 57. As LL fault is an unbalanced fault, there is huge oscillation of torque as observed in every case. For the no controller case, at the fault initiation there is a sudden change of torque. Then it

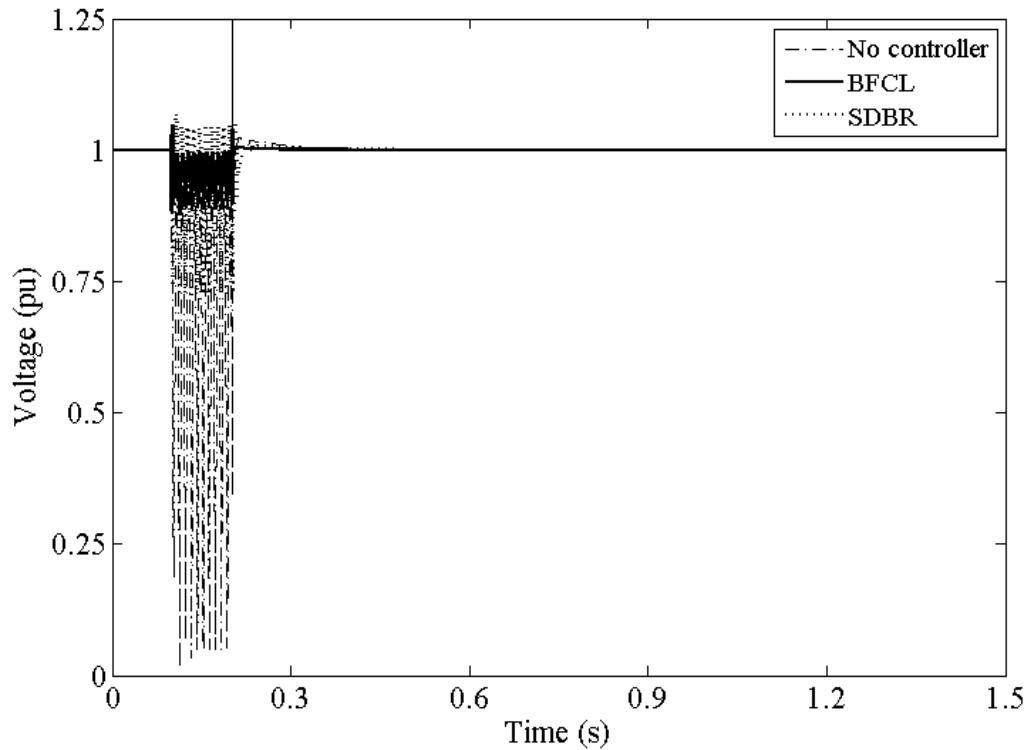


Figure 55. Wind generator terminal voltage for LL fault

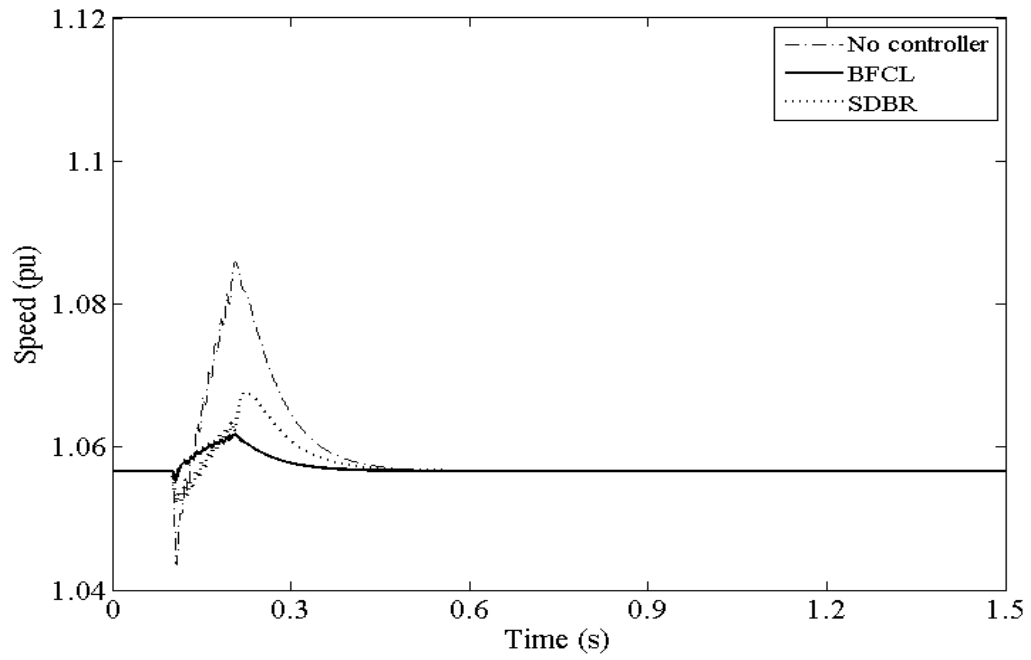


Figure 56. Wind generator speed for LL fault.

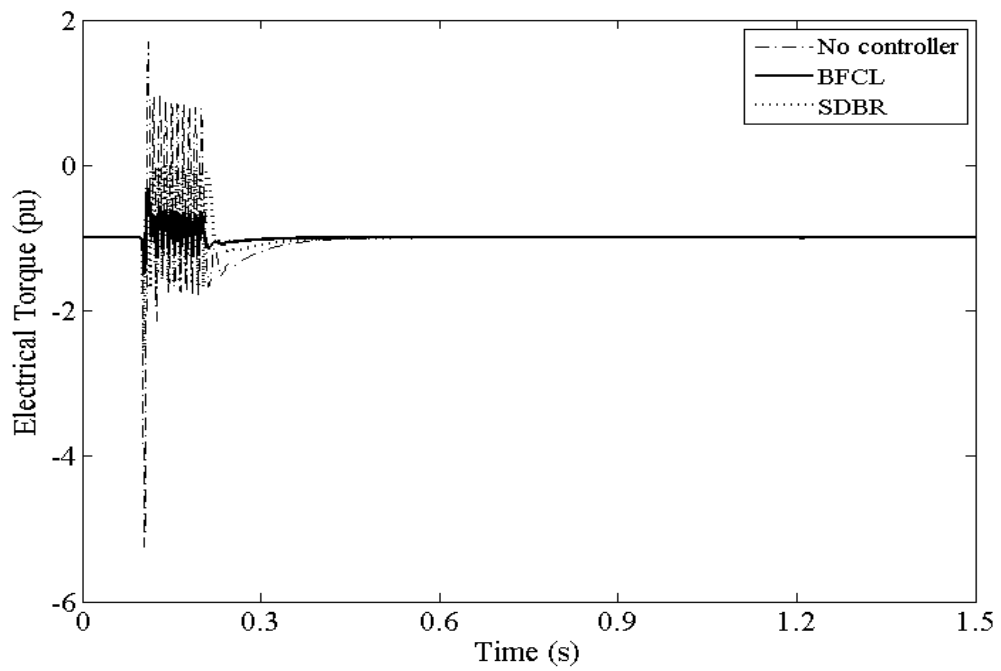


Figure 57. Wind generator electrical torque for LL fault.

oscillates in between 1 to -2pu. This high torque fluctuation is very harmful for turbine generator system. The SDBR has the capability to reduce the magnitude of oscillation in the range of 0 to -1.5pu. When the BFCL is inserted in the system this fluctuation is minimized in between -0.5 to -1.1.

Figure 58 illustrates the active power output at the PCC for LL fault. At the event of LL fault, the power demand at the PCC goes very low. This is shown by the curve for no controller. The power output at the PCC becomes almost zero resulting in increase of wind generator speed. This low power output may cause the wind generator to go unstable in the event of a permanent fault. Also instability may occur if no auxiliary controller is used in the presence of a permanent fault. With the application of BFCL there is no sudden change at the fault or breaker closing instant. The fluctuation is the least. The SDBR shows somewhat better performance than the no controller case, but at the fault instant, the active power jumps to 1.5pu and takes longer time to stabilize as compared to the BFCL.

At the event of fault the system becomes highly inductive. There is huge demand and supply of reactive power at fault and breaker opening instant, respectively. With no controller at PCC there is a reactive power fluctuation ranging from 1 to -1.5pu as apparent from the Figure 59. With the SDBR included in the system, the reactive power demand is not changing that much rapidly and sharply, but at the fault and breaker opening instant there is some exchange of reactive power. The BFCL gives the best performance with the least variation in reactive power at PCC.

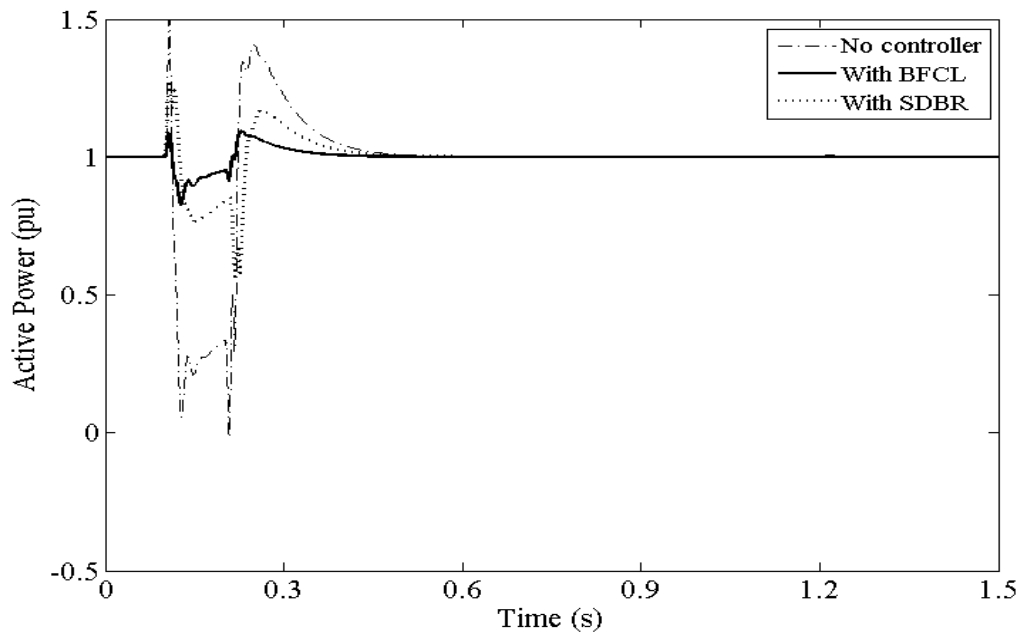


Figure 58. Wind generator active power output at PCC for LL fault.

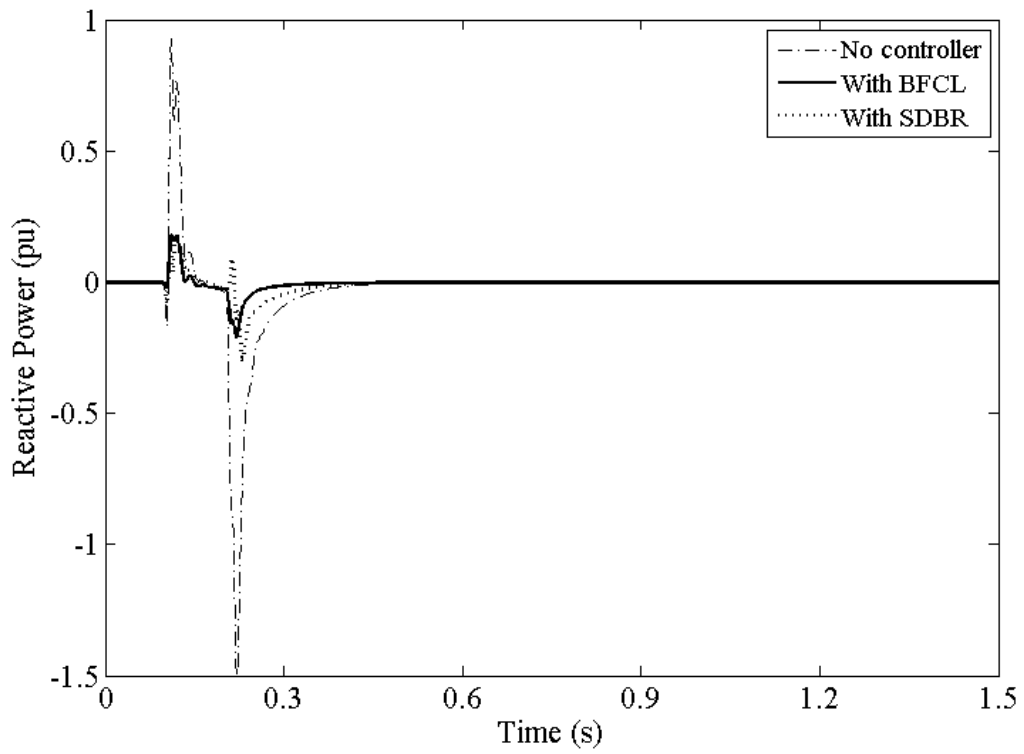


Figure 59. Wind generator reactive power output at PCC for LL fault.

D. Fault Current Suppression and FRT for 1LG Fault

A single line to ground fault is applied to the system at phase a. The obtained responses are given and discussed below.

Fault current into the ground for 1LG fault is given by Figure 60. The BFCL provides the most fault current suppression to around 1.5 pu compared to around 2.5 pu by the no controller case. The SDBR also suppresses the fault current, but its performance is poor compared to the BFCL. Here one thing can be noted. As 1LG is the least severe fault, the fault current doesn't go as high as the 3LG fault case as seen in the Figure 42. This can be easily understood because in 1LG fault only one line is connected to ground and the other two lines are healthy.

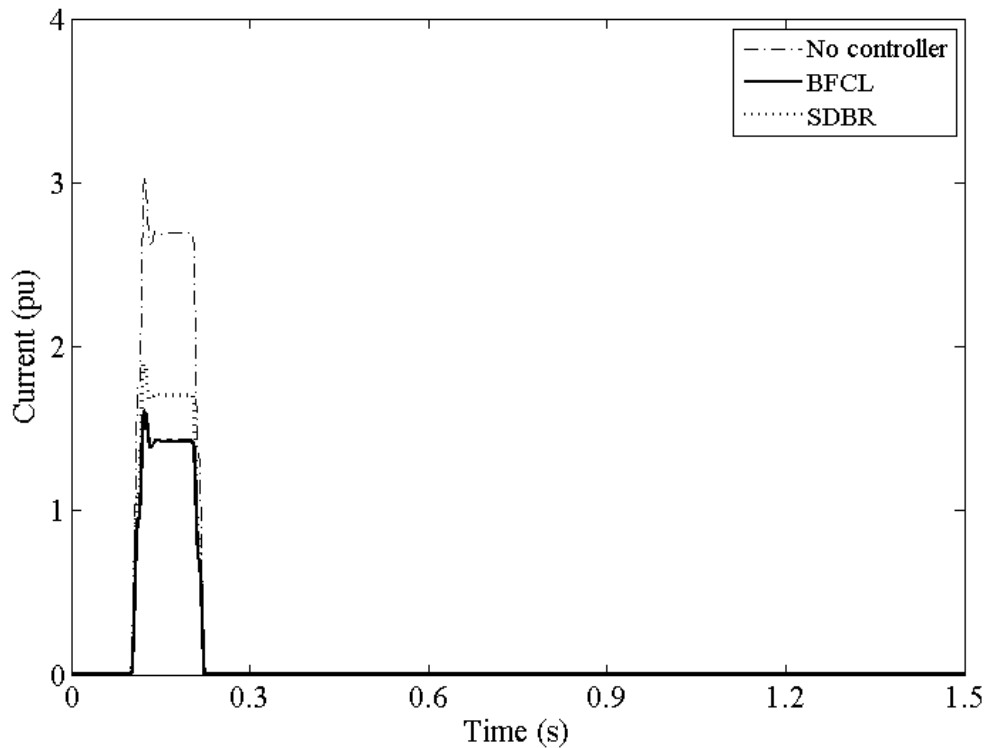


Figure 60. Fault current from line to ground in faulted line for 1LG fault.

The PCC current for the 1LG fault is given in Figure 61. With no controller it rises close to 2 pu and fall down to 0.5 pu at fault. And it stays low until the breaker opening. At breaker opening it again fluctuates. With the SDBR this current rises to 1.25pu and takes longer time to go back to previous value after breaker opening. The BFCL is the best performer here by keeping the fluctuation to $\pm 10\%$ of the nominal value.

The voltage dip at PCC for a single line to ground fault is not so severe compared to that for a 3LG or a LL fault. Without any controller it comes down to around 0.6pu. The SDBR reduces this voltage dip but the BFCL can well keep it to $\pm 10\%$ of the nominal value. This is evident from the Figure 62.

Figure 63 shows the wind generator terminal voltage for 1LG fault. As mentioned earlier, unbalanced faults cause wind generator terminal voltage oscillation. Though the

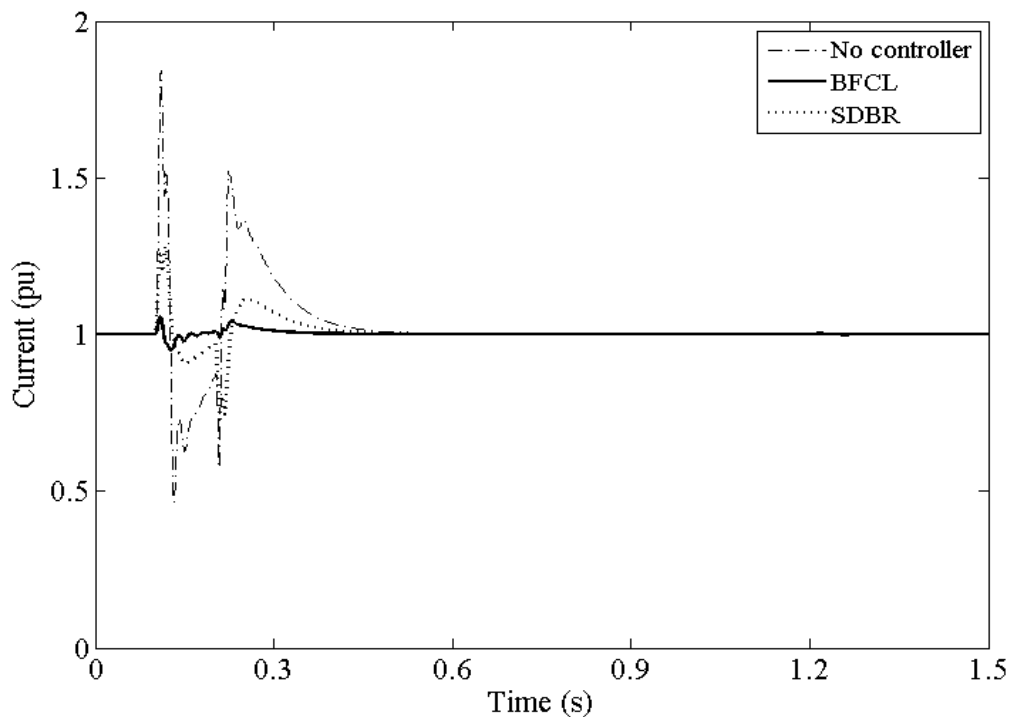


Figure 61. Current at PCC for 1LG fault

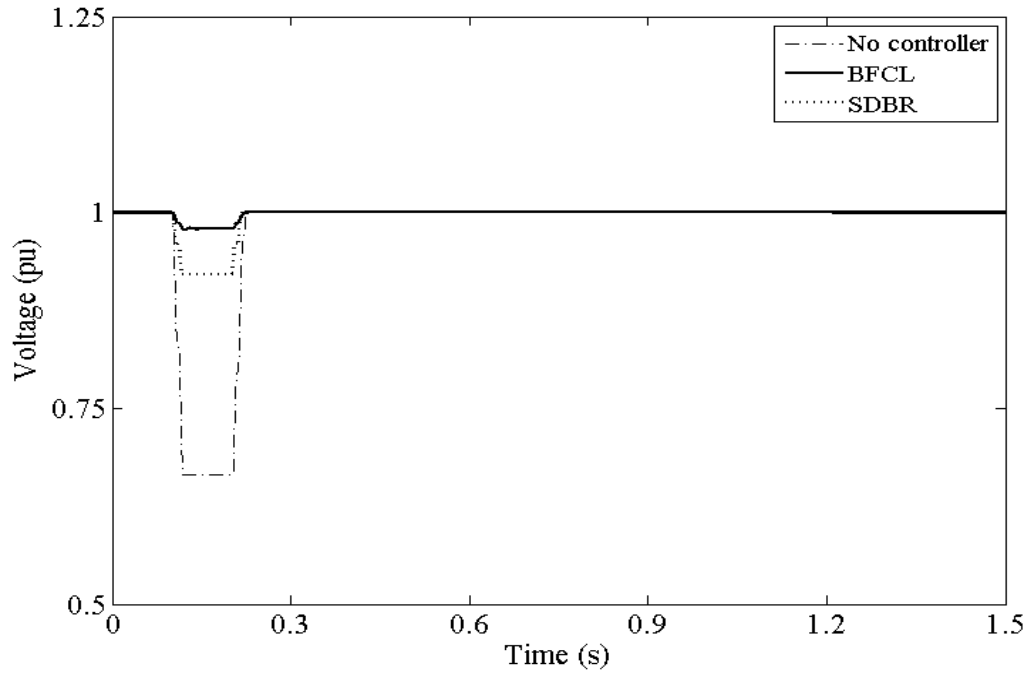


Figure 62. Voltage at PCC for 1LG fault

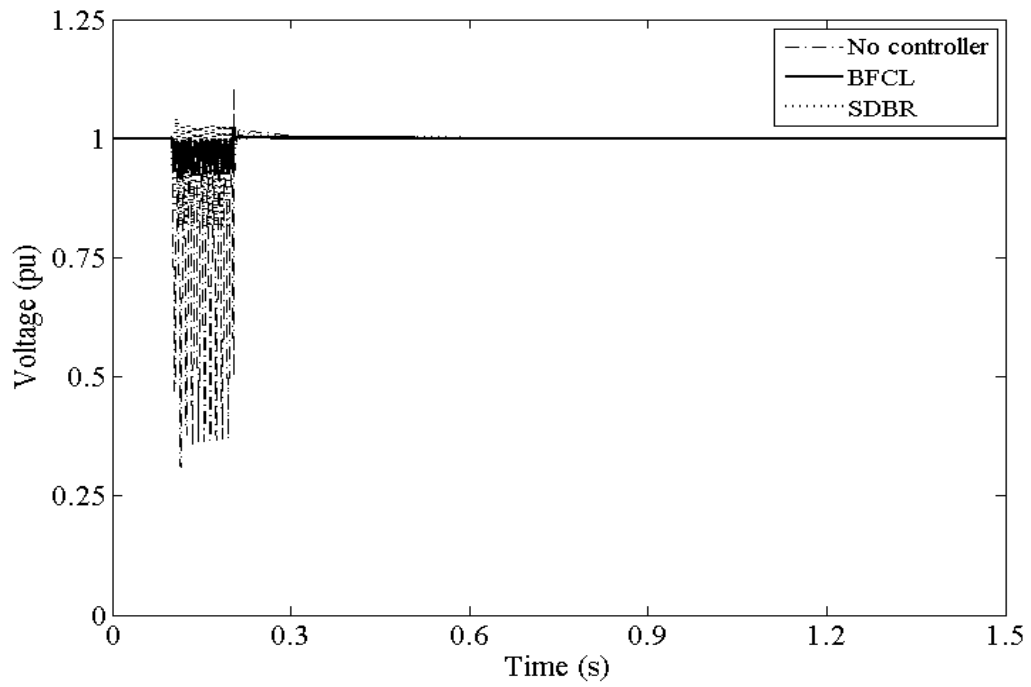


Figure 63. Wind generator terminal voltage for 1LG fault

oscillation for a 1LG fault is less severe than that for a LL fault case, still it is high enough to cause considerable stress on the machine. If no controller is applied, the generator terminal voltage appears to oscillate in between 0.3 to 1.1pu as shown by Figure. The SDBR helps reduce this oscillation range to 0.8 to 1.05pu but the BFCL restricts the oscillation range to 0.9 to 1pu. So it is evident that by the application of BFCL into the system the machine stress is fairly reduced.

Figure 64 shows the per phase voltage waveshapes for three phases corresponding to each of the case considered in this work. As the single phase to ground fault was applied to phase a, the voltage at this phase was dropped down to zero from the fault occurrence instant to the breaker opening as can be seen from the top subfigure, Figure(a). The other two phases are unaffected. The bottom subfigure, Figure(c) shows that the SDBR

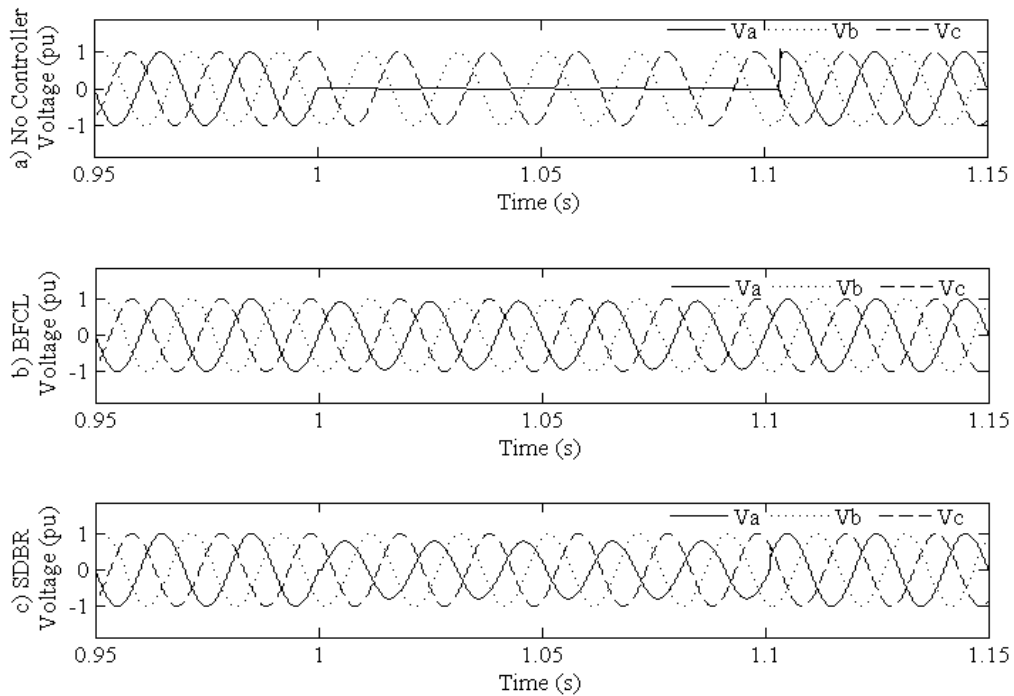


Figure 64. Per phase voltage waveform at PCC for 1LG fault

contributes to keep the phase a voltage unaffected, but still the voltage dip at phase a is visible. Figure 64(b) shows the BFCL performance. It's clear that the BFCL keeps the voltage wave shape almost unaffected. This really helps in reducing harmonic injection at faulted situation.

Figure 65 shows the wind generator speed for 1LG fault. The 1LG fault also makes the wind generator speed go up but the rising rate is not as high as 3LG or LL fault. We can see that with no controller generator speed suddenly goes low and then start to rise. This oscillation creates pressure to machine rotor and turbine generator system. The SDBR restricts the fluctuation to 1% of nominal speed but the BFCL keeps the machine speed almost unchanged, so there is no extra stress on the mechanical system with the BFCL.

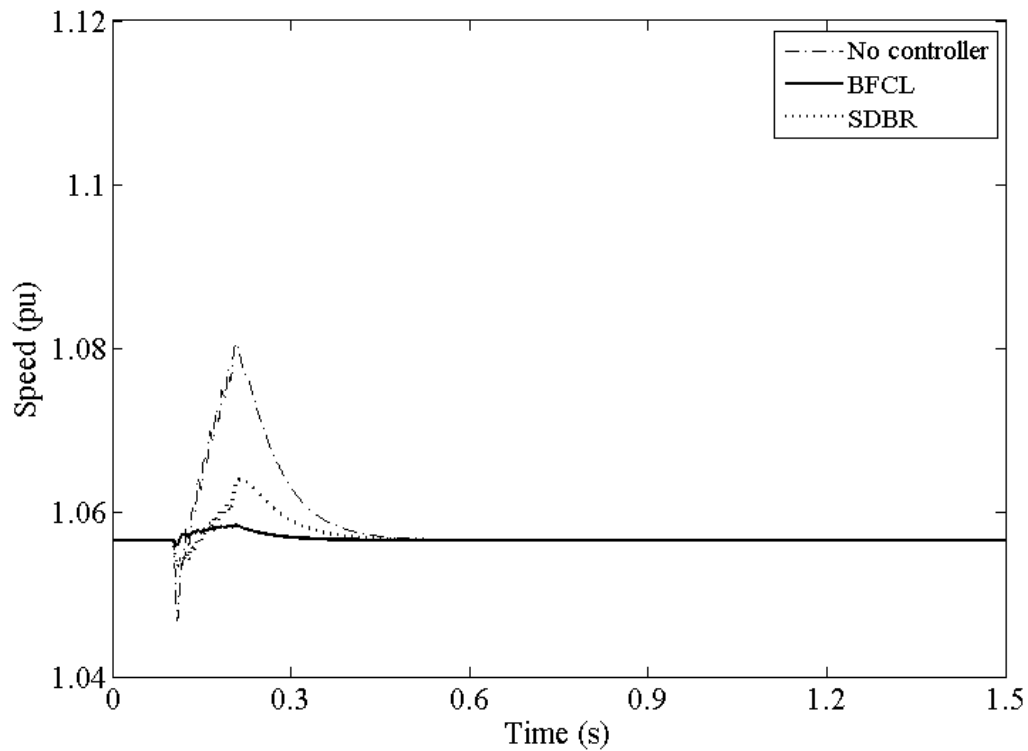


Figure 66. Wind generator speed for 1LG fault.

Figure 66 shows the wind generator torque response for 1LG fault. For this fault there is also oscillation of electrical torque but the oscillation range is narrower than that for the LL fault case. The BFCL almost neutralizes the oscillation. With no controller in action the oscillation range is -1.5 to 1pu and with the SDBR this oscillation is from -0.5 to -1.2pu. Here also, the SDBR performance is inferior to the BFCL.

The BFCL can keep the wind generator active power fluctuation well within $\pm 10\%$ of the nominal active power at the PCC as apparent from the Figure 67. Both the SDBR and no controller case give abrupt change at the fault initiation and breaker opening instant. It is observable that the SDBR performance is better than the no controller case, yet it is not better performer than the BFCL.

The last figure for the 1LG fault is the reactive power response at faulted situation given in Figure 68. With no controller there is abrupt change of reactive power demand

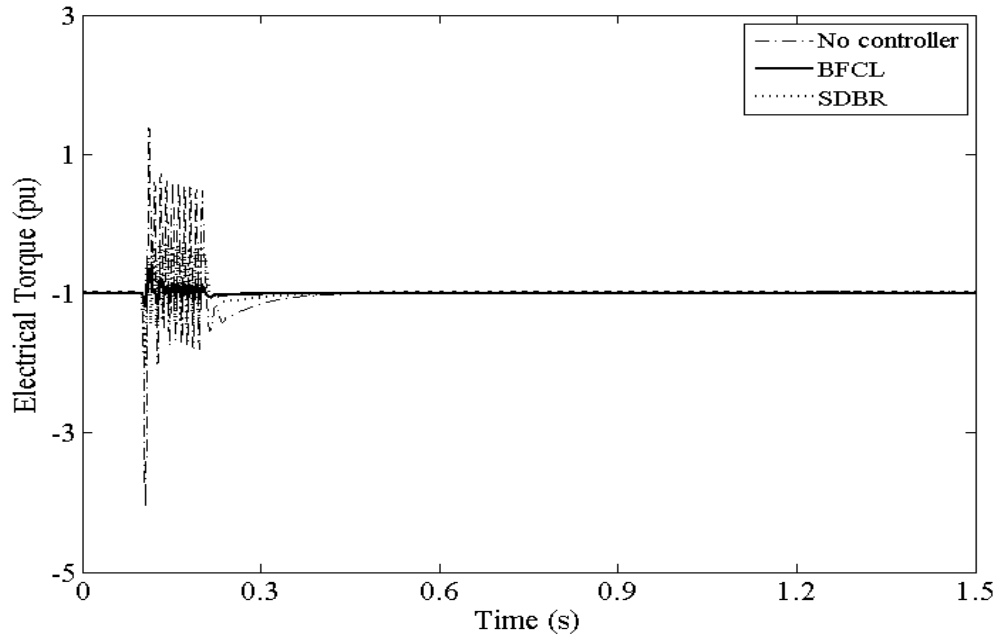


Figure 67. Wind generator electrical torque for 1LG fault.

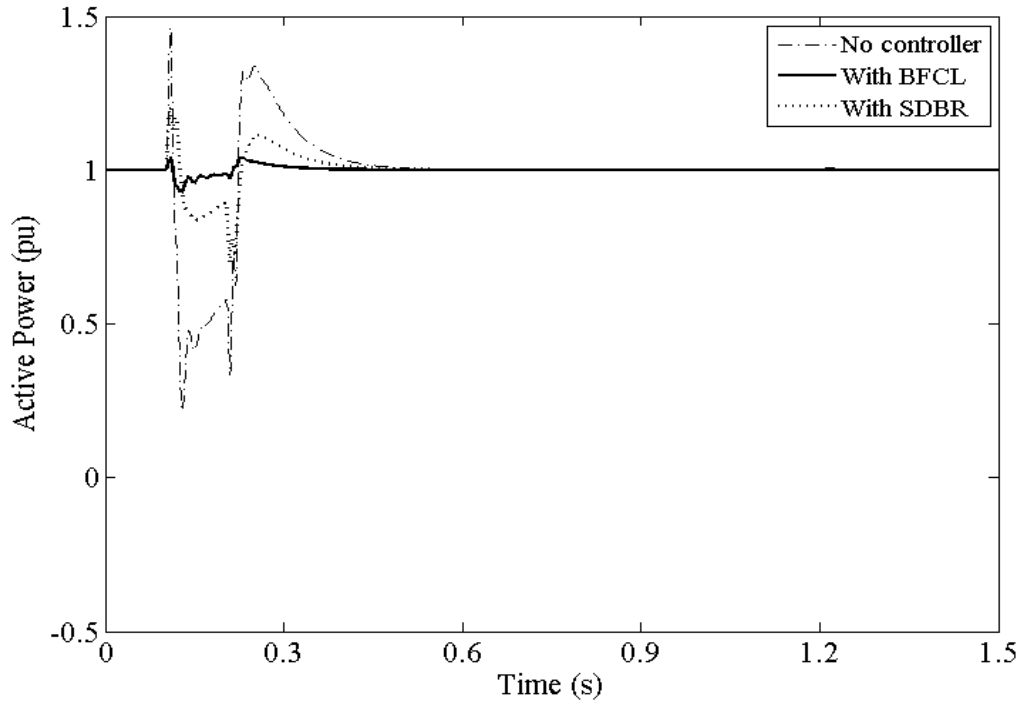


Figure 68. Wind generator active power output at PCC for 1LG fault.

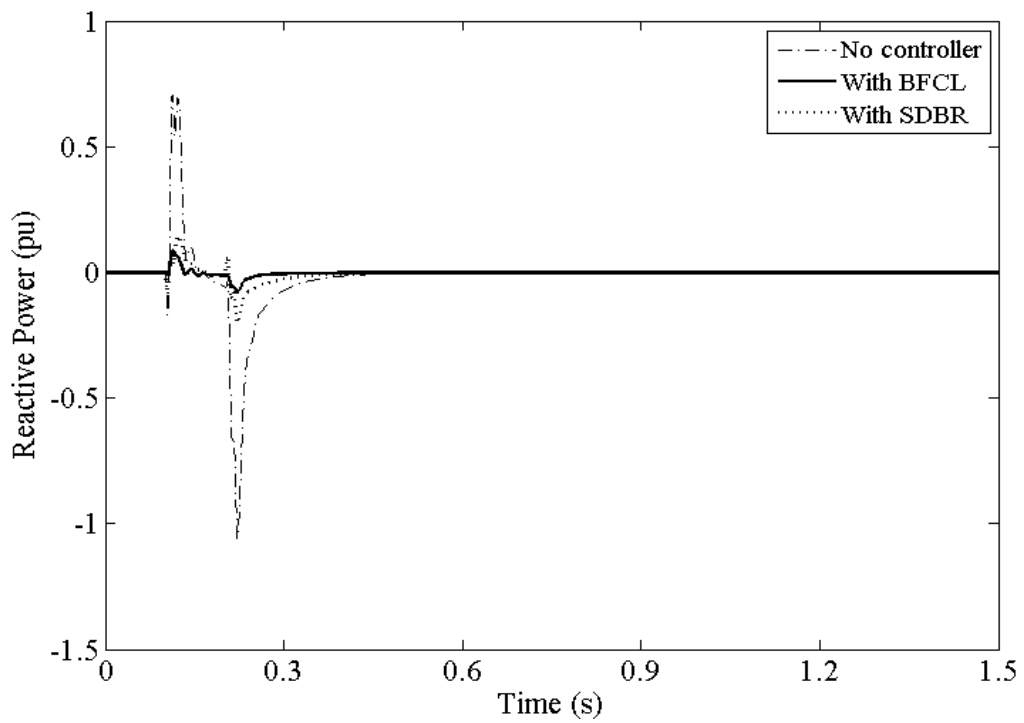


Figure 69. Wind generator reactive power output at PCC for 1LG fault.

and supply at the fault instant as well as the breaker opening instant. Both the SDBR and BFCL show close performance, but the better performance of the BFCL is still noticeable. This also indicates that the BFCL renders better harmonic performance as it prevents the abrupt change of reactive power at PCC.

E. Index Based Comparison

For a clear insight of the performance comparison, several performance indices, namely, $vlt(pu.s)$, $spd(pu.s)$, $pow(pu.s)$, are considered. Lower value of the indices indicates better system's performance. Their definition is given below in equations (17) - (19).

$$vlt(pu.s) = \int_0^T |\Delta V| dt \quad (17)$$

$$spd(pu.s) = \int_0^T |\Delta \omega| dt \quad (18)$$

$$pow(pu.s) = \int_0^T |\Delta P| dt \quad (19)$$

where ΔV , $\Delta \omega$ and ΔP denote the PCC voltage deviation, speed deviation and active power deviation of the wind generator at the PCC, respectively. T refers to the time duration of interest stretching from 0.1s to 1.5s. The values of the indices are presented in tabular form in Tables 11-13. The system performance is the worst without any auxiliary controller. A significant improvement is observed using the BFCL. Compared to the

Table 11. Values of the indices for performance comparison for 3LG fault

Index Parameters	Values of indices		
	No Auxiliary Controller	SDBR	BFCL
$vlt(pu.s)$	3.11	1.12	0.62
$spd(pu.s)$	3.05	1.11	0.63
$pow(pu.s)$	4.23	1.89	1.09

Table 12. Values of the indices for performance comparison for LL fault

Index Parameters	Values of indices		
	No Auxiliary Controller	SDBR	BFCL
$vlt(pu.s)$	1.54	0.39	0.19
$spd(pu.s)$	0.89	0.35	0.16
$pow(pu.s)$	2.96	1.09	0.39

Table 13. Values of the indices for performance comparison for 1LG fault

Index Parameters	Values of indices		
	No Auxiliary Controller	SDBR	BFCL
$vlt(pu.s)$	1.03	0.25	0.11
$spd(pu.s)$	0.73	0.23	0.06
$pow(pu.s)$	2.19	0.72	0.27

SDBR, the BFCL gives lower value of the performance indices for each of the fault types and hence performs better.

This index based comparison really gives a second proof of the BFCL effectiveness and gives another way to compare their performance.

F. Harmonic Study

At the fault initiation and the breaker opening instant, there is huge fluctuation of the demand and generation of the reactive power in the system. Also there are some sudden

switching of network nodes for example circuit breakers. For these reasons a considerable amount of harmonics are injected into the PCC. Along with the grid code, there lies some IEEE standards, for example IEEE 519-1992, which limits the injection of harmonic current and sets benchmark for the total harmonic distortion (THD). THD is the measure of the harmonic presence. Lower value of the THD indicates better system performance. During grid integration, these codes should be followed. The definition of THD is governed by the following equation.

$$THD = \frac{\sqrt{\sum_{h=2}^{h_{\max}} M_h^2}}{M_1} \quad (20)$$

where M refers to voltage or current and h refers to harmonic order.

Table 14 summarizes the harmonic study results for 3LG fault. THD values were calculated using fast fourier transform method. For voltage level of 66KV, the total voltage harmonics should be less than 5% of the fundamental voltage magnitude. For the voltage harmonics, the THD for the BFCL is better than that without auxiliary control and it is below the threshold of 5%. The SDBR also performs better than the no auxiliary control but fails to maintain harmonic threshold level.

Table 14. THD comparison

Total Harmonic Distortion (THD)	Percentage Value of THD		
	No Auxiliary Controller	SDBR	BFCL
THD (V)	13.97	5.05	3.65
THD (I)	15.55	10.1	6.65

The BFCL limits the total current harmonics to 6.65% of the fundamental value, while for the SDBR, it exceeds 10%. So, we can see the BFCL has the ability to improve harmonic performance and limit the voltage THD below threshold limit according to the IEEE standard [65].

G. Implementation Feasibility

The BFCL configuration is based on a few power electronic devices, namely the diode and the IGBT switches. With the advancement in semiconductor fabrication technology, current carrying and reverse voltage withstanding capacity of the diodes and the IGBT switches are higher compared to past. Also now a days, the IGBT can switch at a frequency of 50Khz [66]. So, very fast switching off of the IGBT switch is practically possible.

The probable placement location for the BFCL will be the step up substation of the wind farm. As the controller of BFCL uses local parameters, they can be used in stand-alone as well as the supervisory control and data acquisition (SCADA) controlled system which is very much important for smart grid implementation.

H. Cost Effectiveness of the Proposed Approach

Although the actual cost of the proposed BFCL is not known, but with respect to the number of components used in it, a cost can be guessed. A single phase of BFCL requires 5 diodes, an IGBT, a resistor and an inductor. For high voltage application of diode bridge, a cascaded diode configuration in the bridge arm can be used. Now-a-days, the high current carrying capacity IGBT switches are available and used in rectifier and inverters. Resistors and inductors are basic electrical elements and they are not so expensive like other components, for example transformer. Based on the number of

devices required and their types, it can be concluded that implementation of a BFCL will not be so much expensive if it is compared to a transformer coupled BFCL.

CHAPTER VIII

CONCLUSION

This paper proposes the use of modified BFCL to improve the FRT capability and enhance power quality at the PCC of a FSWT. From the simulation results and discussions, the following points are noteworthy.

- a) The modified BFCL is a very effective means to improve the FRT capacity of fixed speed wind generators.
- b) Suppression of the fault current is achieved by using the BFCL.
- c) Power quality of the system is improved and the voltage harmonic code is maintained by inclusion of BFCL. Moreover, harmonic current is reduced significantly that reduces stress on system components with iron core i.e., the generators and the transformer.
- d) The BFCL prevents huge instantaneous voltage drop at the fault instant, so the generator faces lower stress.
- e) The BFCL minimizes the fluctuation of wind generator speed and enhances stability better than the SDBR.
- f) The BFCL works better than the SDBR in every aspect.
- g) The BFCL is really a cost effective method to enhance FRT capability of the wind generator system.

A. Contributions from the Research

Contribution of this research work is listed below.

- a) A new modified configuration of BFCL is proposed.
- b) Effectiveness of the BFCL for a FSWT system is verified.

- c) The proposed BFCL is equally effective for handling the most severe (3LG) to the least severe (1LG) fault.
- d) Comparative comparison is made with the SDBR, which is a similar technology to the BFCL.
- e) A comparator based controller having multi input parameter handling capability is designed for the BFCL.

CHAPTER IX

FUTURE WORK

This work really paves the way for more research. The potential future works generated by this work, are listed below.

- The performance of the BFCL can be investigated with the variable speed wind generators, such as the doubly fed induction generator (DFIG) and the permanent magnet synchronous generator (PMSG), under the varying wind speed conditions.
- A large power network comprising of many synchronous generators, buses, wind generators, energy storage can be considered, and the FRT of the wind generators can be explored with the BFCL applied to that system.
- Analysis on the multi-mass shaft wind turbine system can be done considering the BFCL presence in the test system.
- The BFCL's performance on the shaft oscillations of the turbine-generator system can be explored.
- Novel topology of the BFCL can be looked for.
- Genetic algorithm (GA) or Adaptive neuro fuzzy inference system (ANFIS) technique can be used for optimization of the BFCL components in a complex system.
- More sophisticated yet simple controller for the BFCL can be designed.
- Nonlinear and robust control for the BFCL can be developed.
- Hardware simulation of the BFCL with wind generator can be done.

REFERENCES

- [1] P. Musgrove, *Wind Power*. New York: Cambridge Univ. Press, 2010.
- [2] T. J. Price, "James Blyth – Britain's first modern wind power pioneer," *Wind Eng.*, vol. 29, no. 3, pp. 191–200, May 2005.
- [3] R. (2012)., *Renewables 2012: Global Status Report*. Paris: REN21 Secretariat.
- [4] "Global Cumulative Installed Capacity 1996-2013." [Online]. Available: http://www.gwec.net/wp-content/uploads/2012/06/02_glob-cum-inst-wcap-96-13.jpg.
- [5] M. H. Ali, *Wind Energy Systems: Solutions for Power Quality and Stabilization*. CRC Press, 2012.
- [6] M. H. Ali, B. Wu, and R. A. Dougal, "An overview of SMES applications in power and energy systems," *IEEE Trans. Sustain. Energy*, vol. 1, no. 1, pp. 38–47.
- [7] M. H. Ali, T. Murata, and J. Tamura, "Minimization of Fluctuations of Line Power and Terminal Voltage of Wind Generator by Fuzzy Logic-Controlled SMES," *Int. Rev. Electr. Eng.*, vol. 1, no. 4, pp. 559–566, Oct. 2006.
- [8] L. Qu and W. Qiao, "Constant Power Control of DFIG Wind Turbines With Supercapacitor Energy Storage," *IEEE Trans. Ind. Appl.*, vol. 47, no. 1, pp. 359–367, Jan. 2011.
- [9] K. Veszpremi and I. Schmidt, "Flywheel Energy Storage Drive for Wind Turbines," in *7th International Conference on Power Electronics and Drive Systems*, 2007, pp. 916 – 923.
- [10] R. B. Schainker, "Executive Overview: Energy Storage Options for a Sustainable Energy Future," in *IEEE Power Engineering Society General Meeting*, 2004, pp. 2309–2314.
- [11] J. G. Slootweg, S. W. H. de Haan, H. Polinder, and W. L. Kling, "General model for representing variable speed wind turbines in power system dynamics simulations," *IEEE Trans. Power Syst.*, vol. 18, no. 1, pp. 144–151, Feb. 2003.
- [12] V. Akhmatov, "Analysis of dynamic behaviour of electric power systems with large amount of wind power," Ph.D. dissertation, Dept. of Electric Power Engineering, Technical University of Denmark, 2003.
- [13] A. D. Hansena and G. Michalke, "Fault ride-through capability of DFIG wind turbines," *Renew. Energy*, vol. 32, no. 9, pp. 1594–1610, Jul. 2007.

- [14] M. Tsili and S. Papathanassiou, "A review of grid code technical requirements for wind farms," *IET Renew. Power Gener.*, vol. 3, no. 3, pp. 308–332, 2009.
- [15] M. Molinas, J. A. Suul, and T. Undeland, "Low Voltage Ride Through of Wind Farms With Cage Generators: STATCOM Versus SVC," *IEEE Trans. Power Electron.*, vol. 23, no. 3, pp. 1104–1117, 2008.
- [16] J. Ren, Y. Hu, Y. Ji, and C. Liu, "Low voltage ride-through control for fixed speed wind generators under grid unbalanced fault," in *Proc. 27th Annual IEEE Applied Power Electronics Conference and Exposition (APEC)*, pp. 686–689.
- [17] T. Senjyu, T. Kinjo, K. Uezato, and H. Fujita, "Terminal voltage and output power control of induction generator by series and parallel compensation using SMES," *Electr. Eng. Japan*, vol. 149, no. 3, pp. 15–23, 2004.
- [18] F. Zhou and L. Joos, G. ; Abbey, C. ; Jiao, "Use of large capacity SMES to improve the power quality and stability of wind farms," in *IEEE Power Engineering Society General Meeting.*, 2004, pp. 2025 – 2030.
- [19] A. Causebrook, D. J. Atkinson, and A. G. Jack, "Fault Ride-Through of Large Wind Farms Using Series Dynamic Braking Resistors (March 2007)," *IEEE Trans. Power Syst.*, vol. 22, no. 3, pp. 966–975, Aug. 2007.
- [20] S. M. Mueen, R. Takahashi, T. Murata, and J. Tamura, "A Variable Speed Wind Turbine Control Strategy to Meet Wind Farm Grid Code Requirements," *IEEE Trans. Power Syst.*, vol. 25, no. 1, pp. 331–340, Feb. 2010.
- [21] D. Ramirez, S. Martinez, C. a. Platero, F. Blazquez, and R. M. de Castro, "Low-Voltage Ride-Through Capability for Wind Generators Based on Dynamic Voltage Restorers," *IEEE Trans. Energy Convers.*, vol. 26, no. 1, pp. 195–203, Mar. 2011.
- [22] A. E. Leon, M. F. Farias, P. E. Battaiotto, J. A. Solsona, and M. I. Valla, "Control Strategy of a DVR to Improve Stability in Wind Farms Using Squirrel-Cage Induction Generators," *IEEE Trans. Power Syst.*, vol. 26, no. 3, pp. 1609–1617, 2011.
- [23] J. A. Wiik, O. J. Fonstelién, and R. Shimada, "A MERS type series FACTS controller for low voltage ride through of induction generators in wind farms," in *Proc. 13th European Conference on Power Electronics and Applications (EPE)*, 2009, pp. 1–10.
- [24] Y. Salami and M. Firouzi, "Dynamic performance of wind farms with bridge-type superconducting fault current limiter in distribution grid," in *Proc. 2nd Int. Conf. . Electric Power and Energy Conver. Syst. (EPECS)*, 2011, pp. 1–6.

- [25] M. Firouzi and G. B. Gharehpetian, "Improving Fault Ride-Through Capability of Fixed-Speed Wind Turbine by Using Bridge-Type Fault Current Limiter," *IEEE Trans. Energy Convers.*, vol. 28, no. 2, pp. 361 – 369, 2013.
- [26] S. M. Muyeen, M. H. Ali, R. Takahashi, T. Murata, and J. Tamura, "Transient Stability Enhancement of Wind Generator by a New Logical Pitch Controller," *IEEJ Trans. Power Energy*, vol. 126, no. 8, pp. 742–752, 2006.
- [27] M. H. Ali and B. Wu, "Comparison of Stabilization Methods for Fixed-Speed Wind Generator Systems," *IEEE Trans. Power Deliv.*, vol. 25, no. 1, pp. 323–331.
- [28] M. Jafari, S. B. Naderi, T. Hagh, M. Abapour, and S. H. Hosseini, "Voltage Sag Compensation of Point of Common Coupling (PCC) Using Fault Current Limiter," *IEEE Trans. Power Deliv.*, vol. 26, no. 4, pp. 2638–2646, 2011.
- [29] S. B. Naderi and M. Jafari, "Impact of Bridge type Fault Current Limiter on Power System," in *Proc. 7th Int. Conf. Electrical and Electronics Engineering(ELECO)*, 2011, pp. 1–4.
- [30] P. S. Flannery and G. Venkataramanan, "A Fault Tolerant Doubly Fed Induction Generator Wind Turbine Using a Parallel Grid Side Rectifier and Series Grid Side Converter," *IEEE Trans. Power Electron.*, vol. 23, no. 3, pp. 1126–1135, May 2008.
- [31] B. Gong, D. Xu, and B. Wu, "Cost effective method for DFIG fault ride-through during symmetrical voltage dip," in *Proc 36th Ann. Conf. on IEEE Ind. Electron. Society*, 2010, pp. 3263–3268.
- [32] K. E. Okedu, S. M. Muyeen, R. Takahashi, and J. Tamura, "Application of SDBR with DFIG to augment wind farm fault ride through," in *International Conference on Electrical Machines and Systems*, 2011, vol. 5, no. 3, pp. 1–6.
- [33] J. Yang, J. Fletcher, and J. O'Reilly, "A series-dynamic-resistor-based converter protection scheme for doubly-fed induction generator during various fault conditions," *IEEE Trans. Energy Convers.*, vol. 25, no. 2, pp. 422–432, 2010.
- [34] G. J. Slootweg, "Wind Power: Modelling and Impact on Power System Dynamics," Delft University of Technology, 2003.
- [35] "Wind turbine power output variation with steady wind speed," *Wind Power Program*, 2014. [Online]. Available: http://www.wind-power-program.com/turbine_characteristics.htm. [Accessed: 14-Jan-14].
- [36] "Wind turbine." [Online]. Available: <http://www.newen.com.au/Wind-Facts/Wind-Facts/Wind-turbine-.asp>. [Accessed: 13-Feb-2014].

- [37] “Wind Turbines.” [Online]. Available: <http://www.alternative-energy-news.info/technology/wind-power/wind-turbines/>.
- [38] IPCC, “Special Report On Renewable Energy,” 2011.
- [39] P. Jamieson, *Innovation in wind turbine design*. England: Wiley, 2011.
- [40] “Wind Energy Basics,” 2014. [Online]. Available: <http://plainswindeis.anl.gov/guide/basics/index.cfm>. [Accessed: 01-Jan-2014].
- [41] “Horizontal Axis Wind Turbine VS Vertical Axis Wind Turbine.” [Online]. Available: <http://www.windturbinestar.com/hawt-vs-vawt.html>.
- [42] *Offshore Wind Energy*. Environmental and Energy Study Institute, 2010.
- [43] “Airborne wind turbine.” [Online]. Available: http://en.wikipedia.org/wiki/Airborne_wind_turbine.
- [44] S. Heier, *Grid Integration of Wind Energy Conversion Systems*, 2nd ed. Wiley, 2006.
- [45] “Wind Farming in Israel,” *CleanTech 2014*, 2014. [Online]. Available: <http://cleantech.mashovgroup.net/en/?????/Wind Farming in Israel/>.
- [46] “Wind Turbine Technologies,” *Green Energy Rhino*, 2014. [Online]. Available: http://www.greenrhinoenergy.com/renewable/wind/wind_technology.php. [Accessed: 01-Jan-2014].
- [47] P. Dvorak, “Twin rotor 11-MW turbine edges closer to physical prototype,” *Wind Power Engineering Development*. [Online]. Available: <http://www.windpowerengineering.com/design/twin-rotor-11-mw-turbine-edges-closer-to-physical-prototype/>. [Accessed: 01-Jan-2014].
- [48] S. M. Muyeen, J. Tamura, and T. Murata, *Stability Augmentation of a Grid-connected Wind Farm*, 1st ed. Springer, 2009, pp. 23–65.
- [49] S. M. Muyeena, Mohd. Hasan Alia, Rion Takahashia, Toshiaki Murataa, Junji Tamuraa, Yuichi Tomakib, Atsushi Sakaharab, “Transient Stability Analysis of Grid Connected Wind Turbine Generator System Considering Multi-Mass Shaft Modeling,” *Electr. Power Components Syst.*, vol. 34, no. 10, pp. 1121–1138, Feb. 2006.
- [50] E. Muyeen, S.M. Ali, M.H. ; Takahashi, R. ; Murata, T. ; Tamura, J. ; Tomaki, Y. ; Sakahara, A. ; Sasano, “Comparative study on transient stability analysis of wind turbine generator system using different drive train models,” *IET Renew. Power Gener.*, vol. 1, no. 2, pp. 131 – 141, 2007.

- [51] Y. X. and Z. T. Wenping Cao, "Wind Turbine Generator Technologies," in *Advances in Wind Power*, R. Carriveau, Ed. Published Online, 2012.
- [52] B.-J. Hansen, L. H., Helle L., Blaabjerg F., Ritchie E., Munk-Nielsen S., Bindner, H., Sørensen, P. and B., "Conceptual Survey of Generators and Power Electronics for Wind Turbines," Denmark, 2001.
- [53] M. G. M. Juan Gimenez Alvarez, "Technical and Regulatory Exigencies for Grid Connection of Wind Generation," in *Wind Farm - Technical Regulations, Potential Estimation and Siting Assessment*, 1st ed., G. O, Ed. Intech, 2011.
- [54] M. P. P. Stavros A. Papathanassiou, "Mechanical Stresses in Fixed-Speed Wind Turbines Due to Network Disturbances," *IEEE Trans. Energy Convers.*, vol. 16, no. 4, pp. 361–367, Dec. 2001.
- [55] T. Ackermann, *Wind power in power systems*. West Sussex, U.K: Wiley, 2005, p. 65.
- [56] S. Heier, *Grid Integration of Wind Energy Conversion System*. New York: Wiley, 1998.
- [57] S. D. S. P.C. Krause, O. Wasynczuk, *Analysis of Electric Machinery and Drive Systems*, 2nd ed. Wiley-IEEE Press, 2002, pp. 141–187.
- [58] C.-M. Ong, *Dynamic Simulation of Electric Machinery: Using Matlab/Simulink*. Prentice Hall, 1998.
- [59] A. Banik and M. Ali, "Comparison between SFCL and TSC for voltage stability enhancement of wind generator system," in *Proc 2013 Innovative Smart Grid Technologies (ISGT), IEEE PES*, pp. 1–6.
- [60] L. Wu, R. Takahashi, M. Nakagawa, T. Murata, and J. Tamura, "A Basic Study of Wind Generator Stabilization with Doubly-Fed Asynchronous Machine," *IEEJ Trans. Power Energy*, vol. 124, no. 9, pp. 1101–1110, 2004.
- [61] C. M. T. Ortolaza and C. G. Torres, "Wind Farm Transient Simulation on ATP," *ece.uprm.edu*.
- [62] "SKNa 402," 2014. [Online]. Available: http://www.semikron.com/products/data/cur/assets/SKNa_402_02632400.pdf. [Accessed: 14-Feb-2014].
- [63] "HVIGBT," 2014. [Online]. Available: <http://www.mitsubishielectric-mesh.com/products/gonglv/hvigbt/>. [Accessed: 14-Feb-2014].

- [64] K. Okedu and S. Muyeen, "Wind farms fault ride through using DFIG with new protection scheme," *IEEE Trans. Sustain. Energy*, vol. 3, no. 2, pp. 242–254, Apr. 2012.
- [65] S. M. Halpin and R. F. Burch, "Harmonic Limit Compliance Evaluations Using IEEE 519-1992." [Online]. Available: www.calvin.edu.
- [66] "6th Generation IGBT Modules (NX-Series)." [Online]. Available: http://sem.mitsubishielectric.eu/products/power_semiconductors/igbt_modules.